Available online at www.sciencedirect.com
SCIENCE DIRECT®
Geomorphology 53 (2003) 45–73
GEOMORPHOLOGY
www.elsevier.com/locate/geomorph

Modeling runoff and runon in a desert shrubland ecosystem, Jornada Basin, New Mexico

David A. Howes[a,*], Athol D. Abrahams[b]

[a] Compliance Services International, 1112 Alexander Avenue, Tacoma, WA 98421, USA
[b] Department of Geography, University at Buffalo, The State University of New York, Buffalo, NY 14261, USA

Received 10 April 2001; received in revised form 4 October 2001; accepted 1 November 2002

Abstract

A new two-dimensional (2D) distributed parameter model is developed to simulate overland flow in two small, semiarid shrubland watersheds in the Jornada Basin, southern New Mexico. The model is event-based and represents the watershed by an array of 1-m^2 cells, in which the cell size is approximately equal to the average area of the shrubs.

In the model, flow directions and volumes are computed by a second-order predictor–corrector finite difference scheme, which is employed to solve the 2D kinematic wave equation. Thus, flow routing is computed implicitly and may vary in response to flow conditions. The model uses only six parameters for which values are obtained from field surveys and rainfall simulation experiments.

The model underpredicts runoff from the watersheds because the measured values of saturated hydraulic conductivity K_s for intershrub areas are too high. The likely reason for this overestimation is that values of K_s were obtained from runoff plot experiments conducted at the beginning of summer on surfaces with degraded seals, whereas most summer storms occur on surfaces that have experienced recent rainfall and have well-developed seals. Model performance is much improved when K_s is treated as a calibration parameter.

The importance of runon infiltration in supplying water to shrubs is investigated for a range of rainfall and antecedent soil moisture conditions. On average, runon infiltration accounts for between 3% and 20% of the total infiltration under a shrub. The most favorable conditions for runon infiltration are an initially wet soil and a low mean rainfall rate.

Keywords: Runoff; Overland flow; Infiltration; Drainage basin; Hydrology

1. Introduction

During the past 150 years, desert shrubs, such as creosotebush (*Larrea tridentata*), mesquite (*Prosopis glandulosa*), and tarbush (*Flourensia cernua*), have invaded large areas of black grama (*Bouteloua eriopoda*) grassland in the American southwest (Buffington and Herbel, 1965; Archer et al., 1988; Gibbens and Beck, 1988). As a result, landscapes that were once grass-covered are now characterized by scattered shrubs with the intershrub areas devoid of vegetation. This vegetation change, which Schlesinger et al. (1990) viewed as a form of desertification, has had major hydrologic, geomorphic, and socioeconomic consequences for the affected areas.

* Corresponding author.
E-mail address: dhowes@complianceservices.com (D.A. Howes).

0169-555X/02/$ - see front matter © 2002 Elsevier Science B.V. All rights reserved.
doi:10.1016/S0169-555X(02)00347-1

A particularly good example of the transition from grassland to shrubland is found in the Jornada Basin, southern New Mexico, where grass cover declined from around 95% in 1858 to <25% in 1963. Because semiarid ecosystems typical of the Jornada Basin are particularly sensitive to the availability of water, an important consideration in the study of these ecosystems is the nature of the rainfall and runoff processes. The Jornada Basin has a mean annual rainfall of 247 mm (Wainwright, in press), which accumulates in two distinct seasons. In winter, frontal storms originating in the northern Pacific bring low intensity rainfall that may last for several days but generally results in little runoff. In summer, monsoonal airflow from the Gulf of Mexico provides the moisture input for convective thunderstorms. These thunderstorms are characterized by high rainfall rates, short durations, and small areal extents, and are responsible for about 60% of the annual rainfall and virtually all of the runoff.

The main runoff process on semiarid hillslopes, such as those found in the Jornada Basin, is Horton overland flow (Horton, 1933). This type of overland flow occurs when the rainfall rate exceeds the infiltration rate. The infiltration excess is initially stored in small surface depressions, but once these depressions are filled, it begins to flow downhill. Overland flow is hydraulically very complex. Flow depths and velocities are highly variable over space due to microtopography (Dunne et al., 1991) and the presence of stones and vegetation (Emmett, 1970, 1978). Over small areas, overland flow may be laminar, turbulent, transitional, or may consist of patches of any of these three flow states (Abrahams et al., 1990).

A principal consequence of the transition from grassland to shrubland is a significant change in the nature of overland flow. On grassland hillslopes, overland flow is dispersed; resistance to flow is high; and flow velocities are low (Abrahams et al., 1994). On shrubland hillslopes, overland flow tends to be more concentrated in character. Most shrubs reside on microtopographic mounds a few centimeters high, which cause overland flow in the bare intershrub areas to concentrate in flow paths that diverge and converge around the shrubs in a complex reticular pattern. These flow concentrations have greater flow velocities and are more erosive than comparable discharges on grassland hillslopes.

The development of shrub mounds is attributed to a number of abiotic and biotic processes (Schlesinger and Pilmanis, 1998). Abiotic processes include the deposition of fine clastic material by wind and differential rainsplash. Differential rainsplash (Carson and Kirkby, 1972; Parsons et al., 1992) refers to the tendency for more sediment to be splashed from intershrub to shrub areas than in the reverse direction because raindrop energy is dissipated by shrub canopies. In shrubland areas that were formerly grassland, the surface (A-) horizon of the grassland soil has been eroded in the intershrub areas, but remnants persist under the larger shrubs. Thus, the mounds under these shrubs are partly erosional and partly depositional (Parsons et al., 1992; Abrahams et al., 1995). Biotic processes include uptake and subsequent recycling of nutrients through the deposition of litter in the area beneath the shrub, digging by rodents (which enhances infiltration) and the funneling of intercepted rainfall to the base of the shrub by stemflow. Since these processes tend to concentrate water and nutrients beneath the shrub canopies, the shrub mounds tend to correspond to ‘‘islands of fertility’’ (Schlesinger et al., 1990) or ‘‘resource islands’’ (Reynolds et al., 1999).

Studies concerned with the supply of water to shrubs tend to focus on the role of interception and stemflow (e.g., Navar and Bryan, 1990; Martinez-Meza and Whitford, 1996; Abrahams et al., manuscript in preparation). Furthermore, plant growth models developed by Reynolds et al. (1997) to simulate the evolution of shrubland ecosytems are based on the assumption that all of the water reaching a shrub originates as rain falling directly onto the shrub. The lateral redistribution of water by overland flow from areas of runoff to areas of runon is widely recognized as being critical to plant production of desert ecosystems (Schlesinger and Jones, 1984; Noy-Meir, 1985). Yet, the role that runon plays in the supply of water and nutrients to individual shrubs has received little attention. This is mainly due to the lack of a suitable model to simulate overland flow at this scale.

A detailed understanding of overland flow is clearly essential for the study of the vegetation change in semiarid environments. Accordingly, the aim of this study is to contribute to this understanding by developing a two-dimensional (2D) distributed parameter

model to simulate overland flow in the creosotebush shrubland of the Jornada Basin. This model is applied to two small watersheds and then used to investigate the importance of runon in supplying water to shrubs.

2. Model development

2.1. Distributed parameter modeling

Distributed parameter modeling is currently the most widely used method of simulating runoff in semiarid environments (e.g., Zhang and Cundy, 1989; Goodrich 1991; Moore and Grayson, 1991; Vertessy et al., 1993; Flanagan and Nearing, 1995; Smith et al., 1995). This approach involves representing a watershed as a set of spatial (distributed) elements and simulating (i) the hydrologic processes operating within each element (i.e., the conversion of rainfall to runoff), and (ii) the flow of water between elements (i.e., runoff throughout the watershed). In the discussion that follows, the term "runoff processes" refers to items (i) and (ii) collectively.

Distributed parameter modeling allows for the detailed representation of the watershed and an accurate description of the runoff processes using physically based relationships. Because the runoff processes are complex, the mathematical descriptions used in distributed parameter models are generally based on simplified assumptions, finite difference approximations of continuous processes, and empirical relationships describing those aspects of the runoff processes that are not well understood (Pickup, 1988).

2.2. Model requirements

In order to accurately simulate overland flow in the Jornada shrubland, a distributed parameter runoff model should meet the following requirements.

(i) The model elements must be small enough to discriminate between shrub and intershrub areas.
(ii) The model must be able to accurately represent the divergence and convergence of flow around individual shrubs.
(iii) The model should contain the optimum number of parameters to describe the runoff processes accurately but not in excessive detail. Where possible, the model parameter values should be obtainable from field experiments conducted at the same scale as the model elements.

These requirements will be discussed in Section 5 below.

2.3. Model development

2.3.1. Kinematic wave approximation

If it is assumed that changes in momentum in overland flow are negligible compared to both the gravitational force (which promotes flow) and the frictional forces (which transmit the frictional effects of the surface into the flow) (Baird, 1997), the flow velocity v may be calculated using a uniform flow approximation, in this case the Darcy–Weisbach equation

$$v = \sqrt{\frac{8ghs}{ff}} \tag{1}$$

where g is the acceleration due to gravity (cm s^{-2}), h is the flow depth (cm), s is the slope, and ff is the *friction factor*. Thus, gradually varied, non-uniform, free-surface flow may be visualized as a succession of steady uniform flows (Chow, 1959; Ponce, 1991). The coupling of a uniform flow equation with the continuity equation produces the kinematic wave approximation to the Saint Venant flow equations (de Saint Venant, 1871; Ponce, 1991)

$$\frac{\partial h}{\partial t} + \frac{\partial q}{\partial x} + \frac{\partial q}{\partial y} = r - f \tag{2}$$

where t is the time (h), x and y are space increments (cm), r is the rainfall rate (cm h^{-1}), f is the infiltration capacity (cm h^{-1}), and q is the unit discharge (cm^2 h^{-1}), which is computed as

$$q = vh. \tag{3}$$

The kinematic wave approximation was proposed by Lighthill and Witham (1955) and first applied to watershed modeling by Henderson and Wooding (1964). Many studies have subsequently utilized this approach to simulate overland flow on a range of

hillslope surfaces (e.g., Woolhiser and Liggett, 1967; Wu et al., 1978; Cundy and Tento, 1985; Goodrich 1991; Scoging et al., 1992; Parsons et al., 1997).

2.3.2. Friction factor

As will be discussed below, field experiments were performed adjacent to the north and south watersheds to establish the value of *ff* for the watershed surfaces. These experiments confirm the findings of other studies conducted on similar surfaces (e.g., Abrahams et al., 1986) which indicate that the value of *ff* varies with the flow rate represented by the dimensionless Reynolds number $Re = 4hv/\nu$, where ν is the kinematic viscosity of the water ($cm^2\ h^{-1}$). However, Abrahams and Parsons (1994) showed that on such surfaces the variation in *ff* due to *Re* is an order of magnitude less than the variation in *ff* due to form resistance (including the effects of microtopography, stone cover, and vegetation cover) and that *ff* can be treated as a constant for a given surface type. Therefore, in agreement with most other runoff models (e.g., Gilley and Weltz, 1995; Smith et al., 1995; Corradini et al., 1998), a fixed value of *ff* is used in the model for each type of surface.

In the kinematic wave approximation, the relationship between q and h is known as the kinematic approximation to the momentum equation (Sherman and Singh, 1976) or the rating equation. This equation has the form

$$q = \alpha h^m \tag{4}$$

where α is the kinematic wave friction relationship parameter ($cm^{2-m}\ h^{-1}$) and m is the slope-friction coefficient. When v is computed using the Darcy–Weisbach equation and s and *ff* are constant, then α and m are both constants and their values can be obtained from Eq. (1) as follows:

$$v = \sqrt{\frac{8ghs}{ff}} = \alpha h^{0.5} \tag{5}$$

where $\alpha = \sqrt{\frac{8gs}{ff}}$. Therefore, from Eq. (3)

$$q = vh = \alpha h^{1.5} \tag{6}$$

Thus, m in Eq. (4) is equal to 1.5.

2.3.3. Infiltration

Infiltration is described in the model using the storage-based Smith–Parlange equation (Smith and Parlange, 1978; Woolhiser et al., 1990)

$$f = \frac{K_s e^{(F/B)}}{(e^{(F/B)} - 1)} \qquad f > 0 \tag{7}$$

where f is the infiltration capacity ($cm\ h^{-1}$), K_s is the saturated hydraulic conductivity ($cm\ h^{-1}$), F is the infiltrated depth (cm), and B is a soil storage parameter (cm) (Freeze, 1980) defined by

$$B = \frac{S^2}{2K_s} \tag{8}$$

where S is the sorptivity ($cm\ h^{-0.5}$) accounting for both capillary suction and initial conditions. A distinction is drawn between two rates that pertain to the infiltration process (Hawkins and Cundy, 1987). The infiltration capacity f is the maximum rate at which water can enter soil, whereas the infiltration rate i is the actual rate at which water enters the soil. The effect of flow depth on the infiltration rate is assumed to be negligible (Schmid, 1989).

If the soil properties are the same throughout the watershed and all points receive the same amount of rainfall, ponding occurs at all points simultaneously. However, most soil properties are highly variable over short distances (e.g., Nielsen et al., 1973; Springer and Cundy, 1987); and this spatial variability may give rise to runon infiltration. Runon infiltration occurs when runoff generated in an upslope area encounters a downslope area where ponding has not occurred. In the latter area, the rainfall excess is still negative, so the soil still has infiltration capacity to satisfy. Some or all of this unsatisfied capacity may be filled by runon. The effect of runon infiltration is to increase the infiltrated depth and thus accelerate ponding, causing runoff to occur earlier than it otherwise would (Scoging et al., 1992).

Using Eq. (7) and allowing for runon infiltration, the infiltration rate is computed as either

$$i = (q_r + r) \qquad \text{for } f > (q_r + r) \tag{9}$$

or

$$i = f \qquad \text{for } f \le (q_r + r)$$

where q_r is the runon per unit surface area ($cm\ h^{-1}$).

2.3.4. Numerical solution scheme

2.3.4.1. Davis algorithm. The spatial and temporal variation in flow depth is simulated in the model by numerical solution of the 2D kinematic wave equation (Eq. (2)) using an explicit second-order accurate predictor–corrector finite difference scheme developed by Davis (1988). The Davis algorithm was originally designed for problems in computational fluid dynamics and provides greater spatial and temporal accuracy than the one-dimensional numerical schemes used previously in modeling overland flow (e.g., Scoging et al., 1992; Parsons et al., 1997). The ability of the algorithm to capture nonlinear shocks and expansion waves smoothly and accurately makes it well suited to modeling the rapidly changing flow conditions typical of the Jornada shrubland. The model developed for the present study represents the first application of the Davis algorithm to modeling overland flow.

The Davis algorithm can be summarized as follows. For each cell in the model grid, the flow depth is calculated at each time step by taking into account the flows between the cell and each of the eight neighboring cells. Flows in the cardinal directions are calculated explicitly, whereas those between the cell and its diagonal neighbors are calculated implicitly. The equations underlying the algorithm are too complex to describe in full in this paper, but the basic approach can be illustrated using simplified versions of the model equations. The simplified numerical scheme discussed below (Eq. (12)) is not stable in its own right but is made stable by minor modifications included in the Davis scheme.

Second-order accuracy in the spatial dimensions is obtained using center-differencing. Accordingly, with the value of the source term $(r-f)$ set to zero, Eq. (2) can be expressed as

$$\frac{h_{i,j}^{t+\Delta t}-h_{i,j}^{t}}{\Delta t}+\frac{q_{i+\Delta x,j}^{t}-q_{i-\Delta x,j}^{t}}{2\Delta x}+\frac{q_{i,j+\Delta y}^{t}-q_{i,j-\Delta y}^{t}}{2\Delta y}=0. \tag{10}$$

If the flow velocity in the x direction is denoted by a and that in the y direction is denoted by b, using Eq. (2), Eq. (10) can be rewritten as

$$\frac{h_{i,j}^{t+\Delta t}-h_{i,j}^{t}}{\Delta t}+\frac{a}{2\Delta x}\left(h_{i+\Delta x,j}^{t}-h_{i-\Delta x,j}^{t}\right)+\frac{b}{2\Delta y}\left(h_{i,j+\Delta y}^{t}-h_{i,j-\Delta y}^{t}\right)=0 \tag{11}$$

which can be solved for h $h_{i,j}^{t+\Delta t}$ to give

$$h_{i,j}^{t+\Delta t}=h_{i,j}^{t}-a\frac{\Delta t}{2\Delta x}\left(h_{i+1,j}^{t}-h_{i-1,j}^{t}\right)-b\frac{\Delta t}{2\Delta y}\left(h_{i,j+1}^{t}-h_{i,j-1}^{t}\right). \tag{12}$$

Second-order accuracy in space is obtained using the midpoint rule in which h for a cell is computed in two steps: (i) at the midpoint of a given time step (the predictor step) and (ii) at the end of the time step (the corrector step).

In the predictor step, h is estimated for each of the four cardinal neighbors of a cell, and these midtime values are used to compute h for the cell in the corrector step

$$h_{i,j}^{t+\Delta t}=h_{i,j}^{t}-a\frac{\Delta t}{2\Delta x}\left(h_{i+1,j}^{t+\Delta t/2}-h_{i-1,j}^{t+\Delta t/2}\right)-b\frac{\Delta t}{2\Delta y}\left(h_{i,j+1}^{t+\Delta t/2}-h_{i,j-1}^{t+\Delta t/2}\right). \tag{13}$$

Thus, the calculation of $h_{i,j}^{t+\Delta t}$ takes into account not only the components of flow along the axes but also the components of flow from the diagonal cells $(i-1,j+1)$, $(i+1,j+1)$, $(i+1,j-1)$ and $(i-1,j-1)$ through the calculation of the midtime h values in the predictor step. Stability of the numerical solution scheme is ensured by the use of the Courant condition and a source term stability measure.

2.3.4.2. Initial and boundary conditions. The value of h is set to zero in all cells at the beginning of a simulation run, and the antecedent moisture is specified by assigning an initial value to F in the Smith–Parlange equation (Eq. (7)). At the end of each time step during a model run, h is set to zero in all cells along the boundary of the model grid. In other words, the boundary cells act as permanent sinks. In general, this procedure is likely to have a negligible effect on the simulation of runoff in the watershed as long as

the boundary cells are several meters from the watershed boundary.

3. Study watersheds

3.1. Introduction

A central feature of the geomorphology of the Jornada Basin is the coalescing alluvial fans or bajadas that project into the basin from the mountains on either side. The bajadas consist of sediments eroded from the mountains and range in slope from 7° at the base of the mountains to 0° in the playa in the center of the basin. Two types of drainage channel are found on the bajadas: (i) large, sand-bedded channels, locally known as arroyos, that head in the mountains, traverse the bajadas, and disperse before reaching the playa; and (ii) smaller channels, herein referred to as rills, that are often discontinuous and/or anastamozing and drain the bajada surface between the arroyos. The watersheds of two such rills were selected for the present study. These watersheds are located in the creosotebush shrubland at the foot of Mount Summerford, the northernmost peak of the Doña Ana Mountains (Fig. 1).

The two watersheds differ slightly in terms of their relief, surface properties, and the nature of the shrubs. These differences, however, are typical of the variation across the creosotebush shrubland at Jornada. The watersheds are referred to as the north and south watersheds.

3.2. North watershed

The north watershed lies ~750 m downslope from Mount Summerford (Fig. 1) and is thought to represent an area that was formerly grassland and has been invaded by creosotebush within the last 150 years. Apart from occasional small forbs, vegetation is generally absent from the intershrub areas. The watershed is 65 m long, has a maximum width of 18 m, and an area of 775 m^2. The range in elevation is 2.30 m, most of which is accounted for by the slope of the bajada surface. As shown in Fig. 2, the slopes in this watershed are gentle.

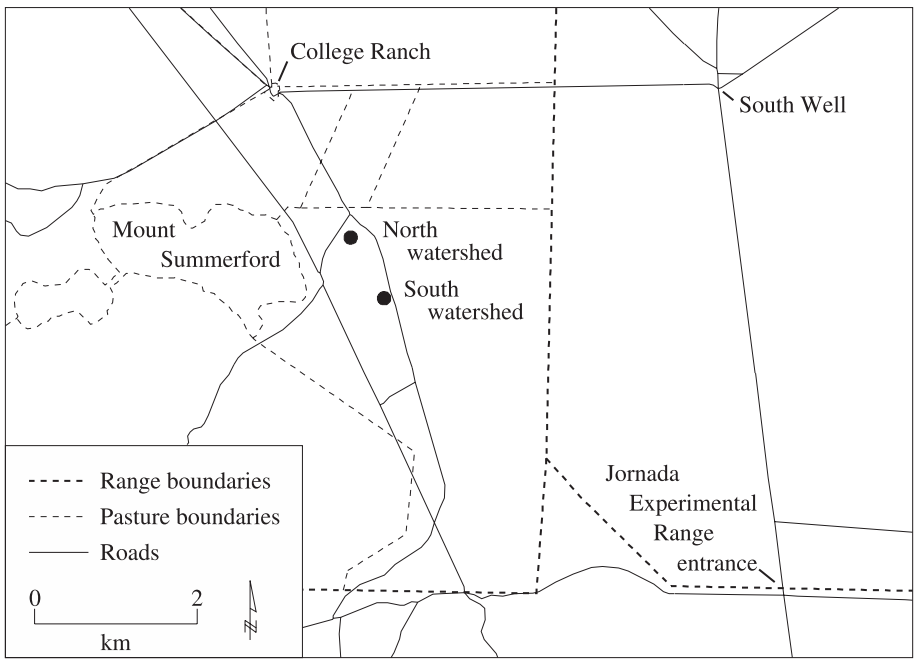

Fig. 1. Location of the north and south watersheds within the Jornada Experimental Range.

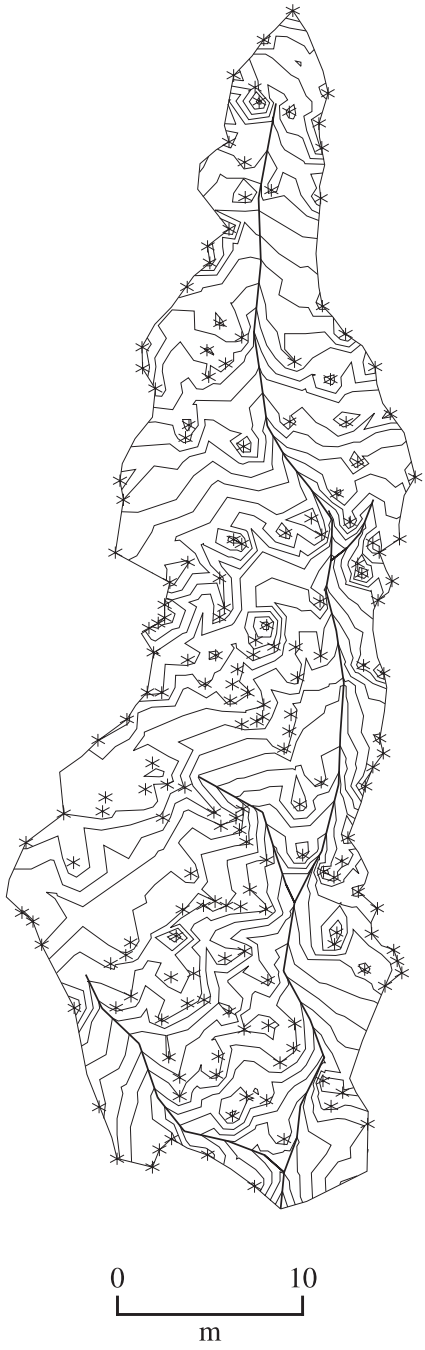

Fig. 2. Map of the north watershed showing 5-cm contours, rills, and shrubs.

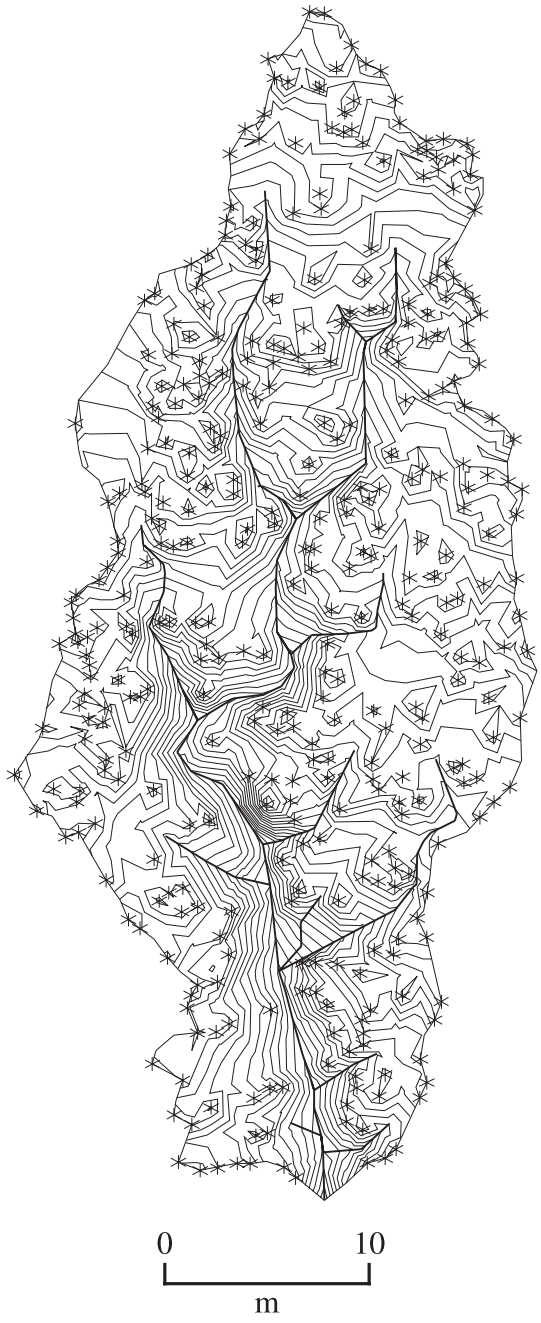

Fig. 3. Map of the south watershed showing 5-cm contours, rills, and shrubs.

The soil underlying the shrub and intershrub surfaces is a Typic Haplargid loamy sand of mid-Holocene age derived from Mount Summerford alluvium

(Schlesinger et al., 1999). The rills have sandy beds that, like the loamy sand, have a gravel content of < 5% (by weight).

All of the shrubs in the north watershed are underlain by the same type of soil, but this soil may be bare, covered by grass (*Muhlenbergia porteri*), or covered by litter. The presence of vegetation or litter increases the friction encountered by water flowing under the shrubs. This increased friction causes a reduction in flow velocity and thus increases the likelihood that the water will infiltrate rather than runoff into the surrounding intershrub area. Since the differences in ground cover affect the amount of runoff in the watershed, the distinction between the three surface types had to be retained in the modeling (see Section 5.2.1).

3.3. South watershed

The south watershed is situated ~ 1.2 km SE of the north watershed (Fig. 1); it is 58 m long, has a maximum width of 23 m, and an area of 889 m^2. As in the north watershed, most of the 2.86-m range in elevation is accounted for by the slope of the bajada surface. However, as Fig. 3 shows, the rill network is more incised than in the north watershed.

The watershed is located on Typic Haplargid soils formed in alluvial igneous materials originating in the Doña Ana Mountains to the south and west of Mount Summerford (Schlesinger et al., 1999). In the main rill, the roots of several shrubs are exposed to depths of up to 30 cm, suggesting that severe erosion has occurred recently. The creosotebush in this watershed are smaller than those in the north watershed and have poorly developed bare mounds. The mounds consist of loamy sand, while the rill beds consist of sand. In contrast to the north watershed, gravel constitutes 30% of the rill and intershrub soils, and 5% of the shrub soil.

4. Model grid

In order to model overland flow using the Davis algorithm, the north and south watersheds were represented by arrays of square cells. Because the runoff processes operating beneath shrubs contrast sharply with those operating between shrubs, each cell was classified as either shrub or intershrub. A cell size of 1 m^2 was chosen to correspond to the average area of the shrub mounds in the south watershed. Although the shrub mounds in the north watershed are about twice as large, the same cell size was used in both watersheds to facilitate comparison of the results.

In distributed parameter modeling, parameter values obtained for a small area are often assigned to model cells representing much larger areas (e.g., Bathurst, 1986). This is problematic because the spatial averaging of model parameters, such as K_s and *ff*, will be greater over a model cell than over the parameterization area (Beven, 1989; Grayson et al., 1992b). The use of 1-m^2 cells in the present study makes it feasible to conduct field experiments to parameterize the model at the same scale as the model cells. This ensures that the spatial averaging of model parameters is the same in the model cells as in reality.

For each watershed, the model grid was aligned with the long axis of the watershed; and the grid was positioned such that the flume at the outlet of the watershed was located in the center of a cell. Simulations with other alignments showed that the major findings were insensitive to grid alignment.

5. Model parameterization

5.1. Introduction

Application of the 2D runoff model to a watershed involves (i) parameterization, (ii) calibration, and (iii) validation. Parameterization refers to the process of assigning known values to parameters for each of the model cells, whereas calibration involves arbitrarily assigning values to the remaining parameters and adjusting them until an acceptable match is obtained between model output and observed data. Using the known and calibrated parameter values, the ability of the model to accurately simulate the runoff from the watersheds can then be tested by running the model for rainfall events other than those used in the calibration process and, for each event, comparing the model hydrograph with the observed hydrograph. This is the process of validation.

Parameterization and calibration of physically based distributed runoff models have been the subject of much discussion. This discussion has centered on

the appropriate number of parameters to be used in such models and, in particular, on the number of parameters that require adjustment during calibration (e.g., Beven, 1989; Grayson et al., 1992b; Refsgaard, 1997). In general, as the number of parameters in a model increases, so too does the potential degree of interdependence between the parameters and, as a consequence, the chance of error. Additionally, as the proportion of the model parameters that require adjustment during calibration increases, the greater is the likelihood that the model output will not be a unique and accurate representation of the runoff process (Beven, 1989). These issues can be addressed in the construction of a runoff model by adherence to the following recommendations (Beven, 1989; Refsgaard and Storm, 1996; Refsgaard, 1997).

(i) The number of parameters should be kept to a minimum.
(ii) Values for as many of the parameters as possible should be determined from field data.
(iii) The parameter values obtained from field experiments should be collected at the same scale as the model elements to which they will be assigned.
(iv) For those parameters that require arbitrary assignment and adjustment, physically acceptable intervals for the parameter values should be estimated from field data or from published sources.

In accordance with these recommendations, the number of parameters employed in the runoff model was limited to six. This number represents a compromise between the need to accurately describe the runoff process and the need to use as few parameters as possible (Beven, 1989). As shown in Table 1, parameter values were acquired from watershed survey data, watershed monitoring data, and rainfall simulation experiments. The procedures used to obtain values for s, K_s, B, and ff are described below, while those for r and F will be discussed in Section 6.

Table 1
Model parameters and the source of their values

Parameter	Symbol	Source
Slope	s	Digital elevation model based on field survey.
Rainfall	r	Tipping bucket rain gauge attached to data logger.
Saturated hydraulic conductivity	K_s	Rainfall simulation experiments.
Soil storage parameter	B	Model fit using rainfall simulation data.
Initial infiltrated depth	F_i	Based on rainfall data.
Darcy–Weisbach *friction factor*	ff	Friction plot experiments or model fit to rainfall simulation data.

5.2. Field methods

5.2.1. Watershed surveys

An important characteristic of the creosotebush shrubland is that very small differences in ground elevation (i.e., the microtopography) can have a significant impact on the pattern of overland flow. Consequently, the ground elevations had to be measured with a high degree of accuracy. This accuracy was achieved by using an electronic Total Station (Pentax PCS-2S) to conduct a detailed topographic survey of each watershed. The survey consisted of all shrub locations and at least one point per square meter in intershrub areas. A 2-m buffer around each watershed was also included in the survey to provide sufficient data to correctly locate the divide. Rills were mapped separately.

Survey points were classified according to the nature of the ground surface. For the north watershed, survey points were classified as either intershrub, shrub with bare mound (shrub-bare), shrub with grass-covered mound (shrub-grass), shrub with litter-covered mound (shrub-litter), or rill. For the south watershed, survey points were classified as simply intershrub, shrub, or rill.

Model grid cells were classified according to these surface types by overlaying the model grid on the survey data. If a cell contained a surveyed point designated shrub and one designated intershrub, the cell was classified as shrub. In the rare event that a north watershed cell contained more than one shrub point, each of which represented a different type of shrub (i.e., bare, grass, or litter), the surface type assigned to the cell was selected at random. In both watersheds, the rills were treated in the same manner as intershrub areas. This protocol

was thought to be reasonable since the rills occupy only a small proportion of the watershed area and the flow is sheet-like.

5.2.2. Watershed monitoring

A supercritical flume was installed at the outlet of each watershed in 1995 and peak discharges were recorded using a calibrated crest-stage gauge placed in a stilling well adjacent to each flume. In 1996, each flume was equipped with an ultrasonic stage recorder (Greyline Instruments Model SLT) to provide flow data for the full duration of each runoff event. Rainfall data for each watershed were obtained from a tipping bucket rain gauge located near the flume. Both the runoff and rainfall data were recorded by a data logger at each site. Power for the instrumentation was provided by heavy-duty batteries, which were kept charged by a solar panel.

5.2.3. Rainfall simulation experiments

5.2.3.1. Rainfall simulator. The rainfall simulator used in this study was developed by Luk et al. (1986) and consisted of two 4.57-m standpipes held vertical by guy ropes. Two SPRACO Cone Jet nozzles were located at the top of each standpipe. The rate of flow through each pair of nozzles was regulated by a gate valve, and the flow pressure measured by a gauge. Water was transported from a local well to the site of each experiment by tanker and pumped to the rainfall simulator using a 3.7-kW pump.

With a flow pressure of 67 kPa, each nozzle supplied rainfall at a rate of 3.6 cm h^{-1}, giving a total of 14.4 cm h^{-1} from all four nozzles. Measurements of drop sizes and calculations of fall velocity indicated that this simulated rainfall had $\sim$ 83% of the kinetic energy of a natural rainstorm of the same intensity (Li and Abrahams, 1999). A rainfall rate of 14.4 cm h^{-1} is not unusual in the Jornada Basin, but it is rare for such a rate to persist for 30 min. Even so, such a duration was necessary in this study to generate measurable amounts of runoff from all shrub and intershrub surfaces. In order to measure the actual rainfall delivered to the surface, rain gauges were evenly distributed on the periphery of each runoff plot. Five gauges were used for each pair of intershrub plots and four were used for each shrub plot.

5.2.3.2. Runoff plot experiments. Thirty runoff plot experiments were performed in the summer of 1996 in order to determine values of saturated hydraulic conductivity K_s and the soil storage parameter B for each type of surface in the north and south watersheds. For each experiment, a runoff plot was constructed with the same shape and area as a model cell (i.e., a 1-m square). Rainfall was applied to the plot for 30 min, and timed runoff samples were collected to generate the discharge hydrograph. The infiltration curve for the plot was obtained by subtracting the discharge from the rainfall rate.

Experiments were conducted on six intershrub plots and four shrub plots at the south watershed, and on 10 intershrub plots and eight shrub plots at the north watershed. Of the eight shrub plots at the north watershed, two had litter-covered ground surfaces, two had grass-covered ground surfaces, and four had bare ground surfaces. The runoff plot experiments were performed outside (but very close to) the watersheds so as to avoid disturbing the watershed surfaces. Sites were chosen that represented the conditions inside the associated watershed as closely as possible. All sites were dry, having received no rainfall for several months prior to the experiments. By conducting experiments on dry soil, the effect of antecedent moisture on the runoff hydrograph was eliminated.

5.2.3.3. Friction plots. Values of *ff* for the intershrub areas were obtained from friction plot experiments adjacent to each watershed. Two friction plots were constructed at the north watershed and three at the south watershed. Each plot was 3 m long and 1 m wide. At the downslope end of each plot, converging walls directed the runoff to a central outflow point. The triangular section so formed was coated with silicone sealant to prevent infiltration. This was necessary to ensure that the discharge at the outflow point was equal to the discharge from a 3-m-long plot. At the upslope end of the plot, a trench was excavated and lined with a plastic sheet. Overland flow was simulated by filling the trench with water released from a pressurized trickle pipe and by allowing the water to overflow from the trench across the full width of the plot. The discharge from the trench (i.e., the inflow to the plot) was determined by measuring the flow pressure in the calibrated trickle pipe. The discharge at the outflow point was measured by

collecting timed volumetric samples. Flow depth across the plot was measured at 5-cm intervals along two strings located 2.0 and 2.1 m from the upslope end of the plot. Different sets of flow conditions were simulated during a run by using a constant rainfall rate and varying the rate of inflow to the plot.

5.3. Field data

5.3.1. Slope

The ArcInfo Geographic Information System package (Environmental Systems Research Institute, 1998) was used to create a Digital Elevation Model (DEM) for each watershed from the survey data, and each DEM was given the same dimensions as the corresponding model grid. The slope data required by the model are generated using an algorithm developed by Tarboton (1997). For every cell in the DEM, a flow vector is calculated for each of eight triangular facets radiating from the center of the cell; and the steepest downslope vector is taken as the flow vector for the cell. The output from the algorithm is an array of x and y slope components.

5.3.2. Saturated hydraulic conductivity

An estimate of K_s was obtained for each runoff plot experiment by fitting the modified Green and Ampt infiltration equation (Green and Ampt, 1911; Scoging and Thornes, 1979) to the infiltration curve using the SAS nonlinear regression procedure (Freund and Littell, 1991). The modified Green and Ampt equation is

$$f = K_s + \frac{b}{t} \tag{14}$$

where f is the infiltration capacity (cm h^{-1}), b is an empirically derived fitting parameter (cm), and t is the time since the start of rainfall (h). Mean values of K_s were computed for each watershed surface type and are presented in Table 2.

An argument may be made that, because the Smith–Parlange equation (Eq. (7)) is used in the model, this equation should also have been used in the estimation of K_s. The modified Green and Ampt equation was used for two reasons. First, the Smith–Parlange equation is more difficult to fit than the modified Green and Ampt equation due to the interdependency of infiltrated depth F and infiltration capacity f in the former equation. Second, the use of the complex Smith–Parlange equation is not necessary because the value of K_s being estimated is the same for both equations. Thus, the simpler, modified Green and Ampt equation was employed to estimate K_s.

5.3.3. Friction factor

Knowing the outflow and inflow rates for the rectangular section of the friction plot, the discharge Q midway between the two graduated strings was estimated by linear interpolation. Such an interpolation assumes that the discharge varies linearly down the plot. Following Abrahams and Parsons (1990), the mean flow depth h was then obtained by averaging the non-zero flow depth readings. Flow velocity was computed by dividing Q by wh, where w is the flow width. The average ground slope at the graduated strings was computed from several measurements made with an electronic level. The value of ff for each set of flow conditions was estimated using a rearranged form of the Darcy–Weisbach equation (Eq. (1))

$$ff = \frac{8g\bar{h}s}{v^2} \tag{15}$$

where g is the acceleration due to gravity (cm h^{-2}), s is the slope, and v is the flow velocity (cm h^{-1}).

Table 2
Mean values for model parameters

Watershed	Surface type	Number of values	$K_s \pm$ S.E (cm h^{-1})	$B \pm$ S.E. (cm)	$ff \pm$ S.E.
North	Intershrub	10	5.81 ± 0.355	1.22 ± 0.201	0.73[a]
	Shrub-bare	3	6.58 ± 0.647	0.55 ± 0.283	0.73[a]
	Shrub-grass	2	8.82 ± 1.219	0.10 ± 0.000	1.00 ± 0.900
	Shrub-litter	3	8.04 ± 1.983	0.13 ± 0.033	1.37 ± 0.857
South	Intershrub	10	2.26 ± 0.681	1.71 ± 0.437	1.08[a]
	Shrub	4	6.49 ± 1.247	0.58 ± 0.074	1.08[a]

[a] Mean of median values obtained from the friction plot experiments.

A constant value of *ff* was obtained for the intershrub surface in each watershed by taking the mean of the median values of *ff* for the intershrub plots. Values for *ff* of 0.73 and 1.08 were obtained for the north and south watersheds, respectively.

Conducting friction plot experiments to obtain a value of *ff* for the surfaces beneath shrub canopies was not practical. However, since the shrub-bare cells in each watershed had similar surface characteristics to the intershrub cells in the watershed, they were assigned the same value of *ff*. This applied to all of the south watershed shrub cells and 61 of the 147 north watershed shrub cells. The values of *ff* for the remaining shrub cells in the north watershed were obtained as part of the procedure for estimating the soil storage parameter *B*.

5.3.4. Soil storage parameter

The value of *B* for a given soil is difficult to obtain by field measurement. Therefore, an attempt was made to obtain an estimate of *B* for the soil corresponding to each of the different surface types in the watersheds using a model-fitting approach based on the data from the runoff plot experiments.

The runoff from the intershrub plots and the shrub-bare plots at each watershed was simulated using the model, with *r*, *s*, K_s, and *ff* being assigned their predetermined values and F_i being set to 0.01 cm to represent dry soil. A series of 30-min simulations was performed to identify the value of *B* that gave the closest match between the simulated and observed hydrographs for the plot (i.e., that for which the root mean square error was least). For the north watershed shrub-grass and shrub-litter plots, the procedure was the same except that *ff* as well as *B* was adjusted. As mentioned earlier, estimating *ff* for these surfaces from plot experiments was not possible. The mean values of *B* for each surface type and *ff* for the shrub-grass and shrub-litter surface types are listed in Table 2.

The suitability of the estimates of *B* can be assessed by referring to Smith and Parlange's (1978, Fig. 1) graph of *B* against initial soil moisture deficit. For a soil with a low clay and silt content, the value of *B* is in the 1–2 cm range, which is consistent with the values obtained from the runoff plot experiments for the loamy sand and sandy loam soils of the north and south watersheds (Table 2).

6. Model calibration

6.1. Parameter values

In order to calibrate the model, cells were assigned values for K_s, *B*, and *ff* determined from the rainfall simulation experiments (Table 2). As discussed earlier, the *x* and *y* components of slope for each cell were generated using the Tarboton algorithm. The only model parameter for which a measured value could not be obtained from field measurement or from published sources was initial infiltrated depth, F_i. A value for F_i must be assigned to each cell to represent the antecedent soil moisture. The approach adopted for specifying this value is discussed below.

6.1.1. Antecedent moisture

For all model cells, F_i was set equal to the depth of rainfall during the 24 h prior to the storm (referred to as prior rainfall). This procedure has a number of weaknesses. For example, it assumes that all prior rainfall infiltrates evenly within the watershed and that soil moisture is not subsequently reduced by evaporation. It also assumes that F_i is not influenced by rainfall more than 24 h prior to a storm. These weaknesses notwithstanding, in the absence of any better procedure, setting F_i equal to the prior rainfall depth is a reasonable option. A sensitivity analysis showed that the model is relatively insensitive to variation in F_i up to 25%. Therefore, modest errors in the estimation of F_i have relatively little effect on the ability of the model to accurately simulate runoff.

6.1.2. Rainfall data

During the period of this study, only four storms generated measurable runoff from the north and south watersheds (Table 3). Of these four storms, two produced small volumes of runoff from the north watershed only (on July 22, 1998 and August 12, 1998), while the other two (on July 30, 1997 and August 14, 1997) generated substantial runoff from both watersheds. The July 30 storm was the biggest of the four with a recurrence interval of 25–30 years (Table 3). It produced runoff over the entire Mount Summerford bajada, and that runoff reached the playa at the foot of the bajada. This was, therefore, a

Table 3
Recorded rainfall and runoff

Watershed	Date of storm	Rainfall				Runoff recordings		Peak runoff		Runoff volume (cm^3)	Prior rainfall[a]	
		Depth (cm)	Start time	End time	Recurrence interval[b] (year)	First time	Last time	Time[c]	Rate (cm^3 s^{-1})		Time since rainfall ended (h)	Depth (cm)
North	7/30/97	1.96	15:59	16:17	30.0	16:04	16:23	10.85	18,491	6,484,245	8.8	1.09
	8/14/97	2.01	18:25	19:00	1.0	18:31	18:58	13.97	10,274	6,685,800	14.5	3.30
	7/22/98	1.22	18:12	18:40	1.5	18:23	18:29	16.42	4,293	1,454,855	N/A	0.01
	8/12/98	1.65	17:29	18:02	1.5	17:36	17:43	10.07	4,849	2,039,925	17.9	0.66
South	7/30/97	1.96	15:58	16:15	25.0	16:01	16:14	6.65	21,806	7,767,918	8.0	1.17
	8/14/97	1.32	18:26	18:58	0.5	18:38	18:57	30.05	4,429	1,808,291	9.8	1.85

[a] Total rainfall during the 24 h prior to the storm.
[b] Based on data from Miller et al. (1973) and Abrahams et al. (in press).
[c] Time since start of rainfall.

significant storm; the kind of storm the model should be able to simulate. Accordingly, this storm is used to calibrate the model.

The July 30, 1997 storm originated as two convective cells that collided south of the study area and moved northward. Rainfall began at the south watershed at 3:58 p.m., reached a peak rate of 16.80 cm h^{-1} after 5 min, and ended after 17 min (Fig. 4; Table 3). At the north watershed, rainfall began at 3:59 p.m., reached a peak rate of 21.30 cm h^{-1} after 8 min, and ended after 19 min (Fig. 5). Considerable runoff occurred in both watersheds, with a peak runoff rate of 21,806 cm^3 s^{-1} in the south watershed and 18,491 cm^3 s^{-1} in the north watershed. Peak runoff occurred within 1–2 min of peak rainfall.

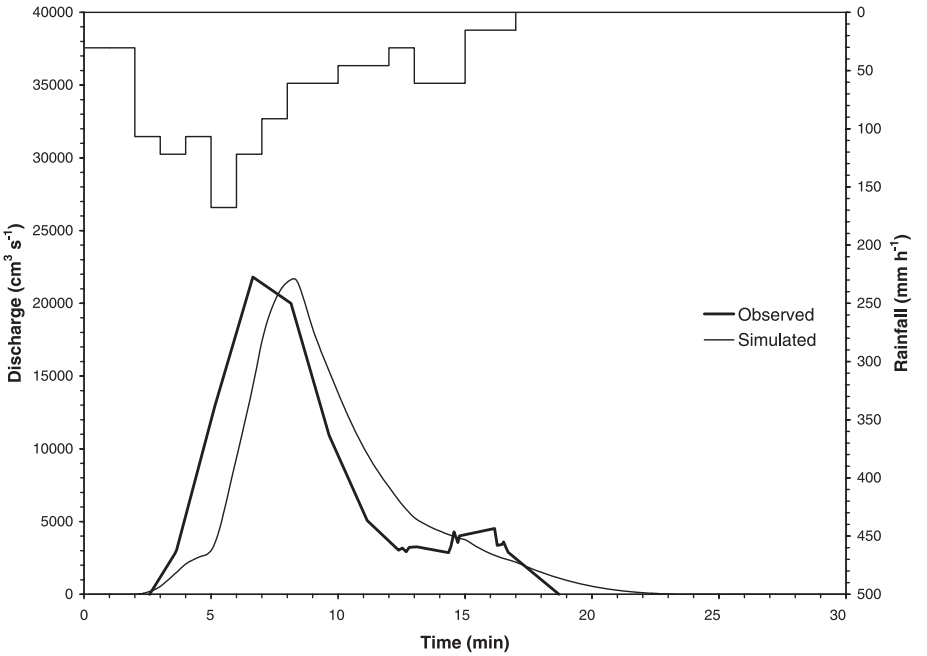

Fig. 4. South watershed observed and simulated hydrographs for the initial calibration runs using the July 30, 1997 rainfall data.

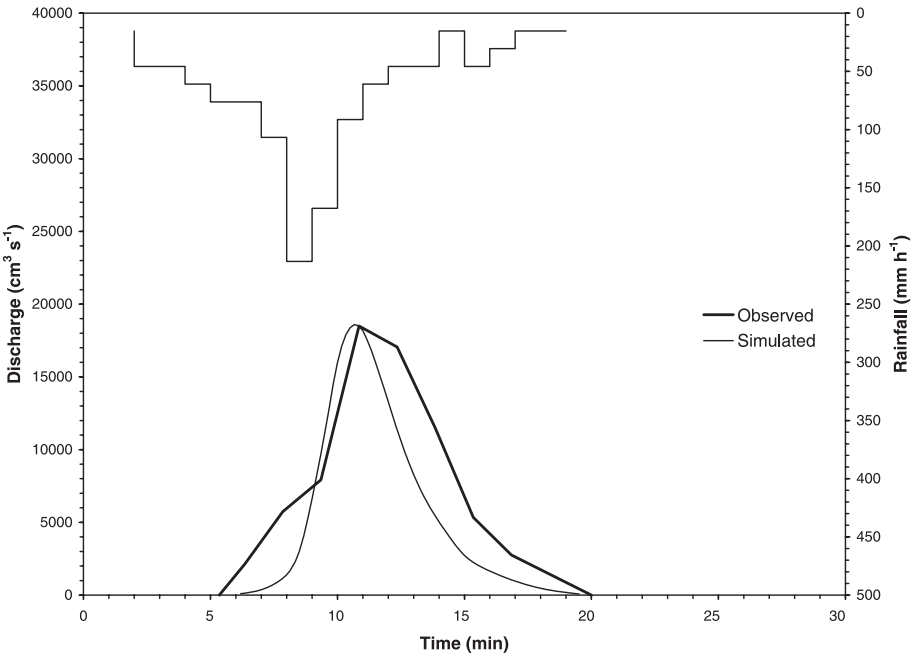

Fig. 5. North watershed observed and simulated hydrographs for the initial calibration runs using the July 30, 1997 rainfall data.

6.2. Initial calibration runs

Initial calibration runs using the July 30, 1997 rainfall data showed that the model underestimated the volume of runoff from the north watershed by 60% and from the south watershed by 18% (Tables 3 and 4). Although the values of F_i, B, K_s, and ff appear to be appropriate for the soil conditions in the watersheds, it was reasoned (i) that since K_s exerts a greater influence on the total volume of infiltration than does either F_i or B, in all probability the measured values of K_s were too high; and (ii) that this discrepancy was presumably related to surface sealing.

6.3. Surface sealing

The term "surface sealing" refers to the development of a thin, relatively impermeable layer at the soil surface. This layer can range in thickness from 0.1 mm to a few millimeters (McIntyre, 1958) and can cause a decrease in infiltrability and an increase in surface runoff. Surface sealing usually occurs on exposed soil surfaces during rainstorms as a result of a number of processes (Moore, 1981; Thompson and James, 1985; Römkens et al., 1990; Poesen, 1992). For example, raindrops impacting the soil surface may compress the soil matrix and disperse soil aggregates, thus releasing fine particles that are drawn into and then block pore spaces in the soil. Fine particles may also be released due to the disintegration of soil aggregates upon wetting.

The development of a surface seal depends on a number of factors, including the kinetic energy of the rainfall, the soil texture, and the stability of the soil aggregates (Moore, 1981; Mohammed and Kohl, 1987). Poesen (1987, 1992) suggested that soils consisting of 90% sand and 10% silt (i.e., sandy loam) are highly susceptible to sealing. Also susceptible are sediments consisting of 80–94% sand and 6–20% silt and clay (i.e., loamy sand). Surface sealing is therefore an important process that can affect both the sandy loam and loamy sand soils found in the north and south watersheds. Surface seals are likely to be less well developed beneath shrub canopies than in intershrub areas due to the attenuation of raindrop energy by the canopy (Wainwright et al., 1999).

The persistence of surface seals following a rainfall event depends on the degree of disturbance of the soil

surface. In the Jornada shrubland, small mammals frequently disturb the soil surface and often destroy the seal. Neave (in press) collected penetrometer data for sealed intershrub surfaces before and after disturbance and showed that the penetration resistance was significantly greater prior to the disturbance than afterwards. In general, the longer the period between rainfall events, the greater is the opportunity for disturbance and the lower is the potential effect of the seal on the runoff processes in a subsequent rainfall event.

6.4. Surface sealing and the runoff plot experiments

In the runoff plot experiments, rainfall was delivered to each plot at a rate of 14.4 cm h^{-1} for 30 min. Since this corresponds to a major storm event in the Jornada Basin, it was expected (i) that seals formed on the intershrub plot surfaces during the 30 min would be as well, if not better, developed compared to seals formed during natural rainfall events, and (ii) that the measured values of K_s would be consistent with these well-developed seals. The measured values were therefore expected to be equal to or less than values of K_s for natural events. However, the initial model results suggest that this is not the case and that the actual values of K_s during the July 30 storm were less than values measured by the experiments. The most likely explanation for the lower than expected values of K_s during the July 30 storm is that seals were better developed prior to the storm than prior to the runoff plot experiments. The experiments were conducted on dry soil after several months without rain. During this interval, the extant seals would have become degraded by drying, cracking, and animal digging. In contrast, the July 30 storm was preceded by several smaller rainfall events, which meant that seals were likely to have been relatively undisturbed at the start of the storm.

6.5. Surface sealing and runoff modeling

Seal development and its effect on K_s present two significant difficulties with respect to runoff modeling. First, K_s values can vary significantly as the seals develop during a storm, with the degree of seal development being dependent on the nature of the storm. Second, it is extremely difficult to estimate the degree of seal development and, hence, the appropriate value of K_s on watershed surfaces at the beginning of a storm.

Grayson et al. (1992a) also found that measured values of K_s were too high compared to actual values in their application of THALES to the Lucky Hills 104 (LH104) catchment at Walnut Gulch Experimental watershed in southern Arizona. Values of K_s for the watershed were obtained from field experiments used in the development of WEPP (Flanagan and Nearing, 1995). In order to achieve satisfactory model results, these values of K_s had to be corrected twice. The first correction reduced K_s to allow for the effects of erosion pavement, vegetation cover, and sealing; while the second correction was an optimizing constant proposed by Goodrich (1990) in the application of KINEROS (Smith et al., 1995) to the LH104 catchment. This second correction was initially set equal to 0.45 but was reduced to 0.16 in order to improve model performance. The magnitude of this correction emphasizes the magnitude of the effect of surface sealing on K_s.

6.6. Final calibration runs

If the discrepancies between the observed and simulated hydrographs for the north and south watersheds are due to surface sealing causing actual K_s values to be lower than measured values, the use of lower K_s values for intershrub cells can be expected to lead to an improvement in the model performance. In order to explore this possibility, K_s was treated as a calibration parameter, and a series of simulation runs was performed to establish the intershrub K_s values that yielded the best model fit for each watershed. The values of the remaining parameters were not changed for these runs.

The best model fits were obtained using $K_s = 3.40$ cm h^{-1} for the north watershed (Fig. 5 and Table 4), and $K_s = 1.60$ cm h^{-1} for the south watershed (Fig. 4). The need to reduce K_s by 2.41 cm h^{-1} (41%) for the north watershed as opposed to 0.66 cm h^{-1} (29%) for the south watershed is consistent with the lower potential for surface seal development in the south watershed owing to the greater stone cover. Fig. 5 shows that for the north watershed the timing of the simulated peak runoff closely matches that of the observed peak runoff, although the runoff volume is

Table 4
Simulated runoff data for application and calibration runs[a]

Watershed	Date	K_s (cm h^{-1})	F_i (cm)	R_v (cm^3)	Q_p		Q_v (cm^3)	Q_c
					Time (min)	Rate (cm^3 s^{-1})		
North	7/30/97[b]	5.81	1.09	15,269,348	11.15	11,985	2,567,809	0.17
	7/30/97	3.40	1.09	15,282,425	10.70	18,599	4,498,493	0.29
	8/14/97	0.30	3.30	15,691,575	29.98	9904	8,326,426	0.53
	7/22/98	0.80	0.01	9,513,734	17.10	4497	1,528,559	0.16
	8/12/98	2.60	0.66	12,694,071	11.74	4775	1,827,808	0.14
South	7/30/97[b]	2.26	1.17	17,556,484	8.43	19,481	6,391,370	0.36
	7/30/97[b]	1.60	1.17	17,553,666	8.27	21,705	7,520,748	0.43
	7/30/97	1.60	1.17	17,558,269	7.88	22,363	7,562,878	0.43
	8/14/97	1.10	1.85	11,884,844	32.24	4349	2,010,483	0.17

[a] Symbols: F_i is initial infiltrated depth, R_v is rainfall volume, Q_p is peak discharge, Q_v is runoff volume, Q_c is runoff coefficient.
[b] Initial simulation runs based on parameter values listed in Table 2 and in this table. All other data based on parameter values listed in Table 5 and in this table.

underestimated by about 31%. The simulated hydrograph for the south watershed (Fig. 4) is similar in shape to the observed hydrograph, but the delay of 1–2 min in peak runoff suggests that the values of *ff* used in the simulation are too high. An alternative approach to determining *ff* for the south watershed surfaces was therefore adopted in the hope that this would yield lower and more suitable values for this parameter.

New values of *ff* were determined for the intershrub and shrub-bare surfaces in the south watershed using the same fitting procedure as was used to estimate *ff* for the north watershed shrub-grass and shrub-litter surfaces. These new values are listed in Table 5, which gives the updated set of parameter values employed in the calibration runs. The values for *B* were also recomputed as part of the fitting procedure, but the new values were very similar to the original values given in Table 2.

As Fig. 6 shows, using the new values of *ff* and *B*, the simulated hydrograph for the south watershed matches the observed hydrograph more closely than was previously the case, although the model is unable to simulate the small secondary peak in the runoff toward the end of the storm event.

6.7. Model parameterization, calibration, and validation issues

The initial attempts to parameterize and calibrate the 2D model for the Jornada shrubland watersheds raise important issues with respect to model parameterization and calibration. Taken together, model parameterization and calibration are traditionally perceived as the process of obtaining a single characteristic set of parameter values that describe the hydrologic properties of a watershed. The predictive capability of a model is usually assessed

Table 5
Updated model parameter values used in simulation runs

Watershed	Surface type	Percentage of watershed area	Number of values	K_s (cm h^{-1})	B (cm)	*ff*
North	Intershrub	81.18	10	[a]	1.22	0.73[b]
	Shrub-bare	11.01	3	6.58	0.55	0.73[b]
	Shrub-grass	2.18	2	8.82	0.10	1.00
	Shrub-litter	5.63	3	8.04	0.13	1.37
South	Intershrub	68.15	10	[a]	1.77	0.58
	Shrub	31.85	4	6.49	0.63	0.38

[a] Individual values for each rainfall event are listed in Table 4.
[b] Mean of three median values obtained from the friction plot experiments.

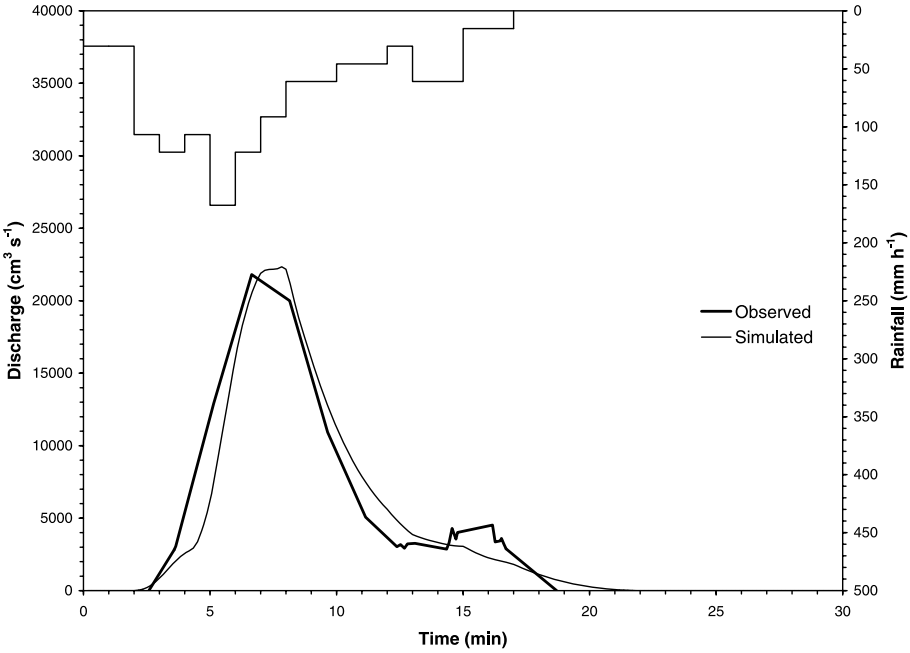

Fig. 6. South watershed observed and simulated hydrographs for the initial calibration runs using the July 30, 1997 rainfall data and the new values of *ff* listed in Table 5.

during model validation by comparing observed hydrographs for a number of storm events with hydrographs simulated using this characteristic set of parameter values. The important assumption in this traditional approach is that the characteristic set of parameter values obtained during model calibration provides an accurate description of the hydrologic properties of a watershed at any time. This assumption, however, is untenable in the case of shrubland watersheds in the Jornada Basin because surface sealing has the potential to dramatically alter the value of K_s in intershrub areas from one storm to the next. Therefore, in the same way that a method is required to estimate F_i for every rainfall event, a procedure is also required to estimate K_s for each event. A procedure may be developed by identifying the values of K_s that give rise to the best fit between the simulated and observed hydrographs for a range of rainfall events in a particular watershed and then relating those values of K_s to the controls of surface sealing. Unfortunately, development of such a relation was not possible in this study due to the scarcity of runoff events. As discussed earlier, apart from the July 30, 1997 storm, measurable runoff from the south watershed occurred on only one occasion and from the north watershed on only three occasions. In the absence of a procedure to accurately estimate K_s for each storm, model validation was not possible. Nevertheless, the rainfall data for these additional storms can be used to demonstrate the ability of the model to simulate runoff from the watersheds.

6.8. Calibration runs using data for other storms

Calibration runs for the additional storms were performed using the values of B, F_i, and *ff* listed in Table 5. Table 4 provides the values of K_s assigned to the intershrub cells in both watersheds in order to achieve the model fits shown in Figs. 7–10. The agreement between the simulated and observed hydrographs is quite encouraging, especially in view of the difficulty of obtaining appropriate parameter values. Having demonstrated that the 2D model simulates reasonably well the runoff from the north and south watersheds, this model is now used to investigate the importance of runon infiltration under shrubs.

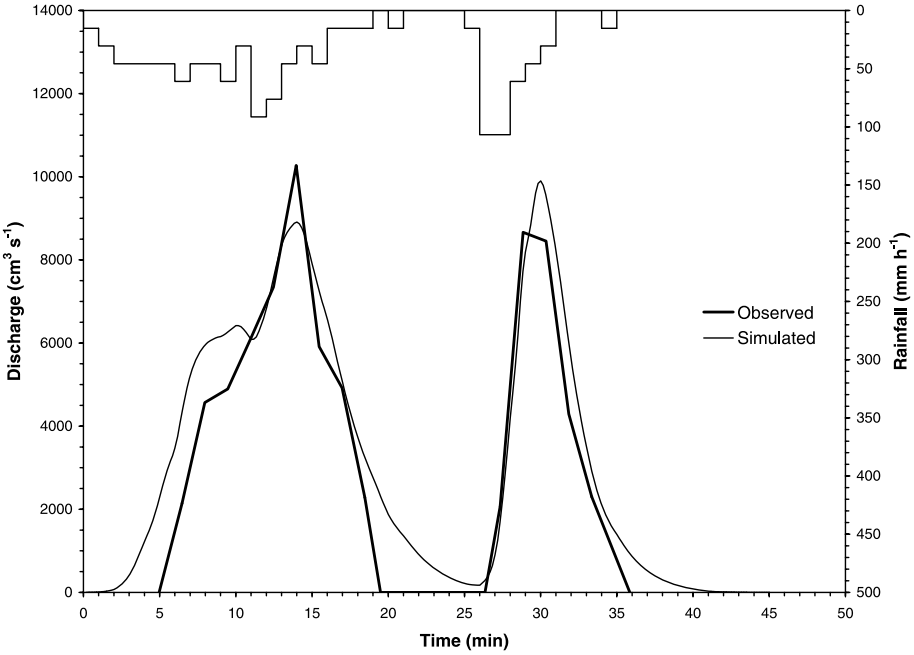

Fig. 7. North watershed observed and simulated hydrographs for the August 14, 1997 storm.

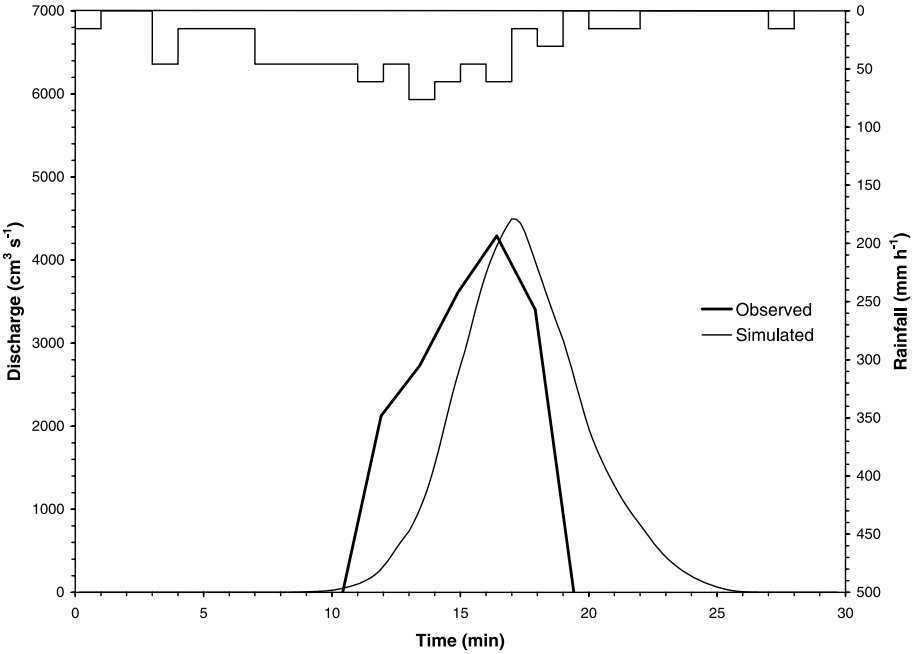

Fig. 8. North watershed observed and simulated hydrographs for the July 22, 1998 storm.

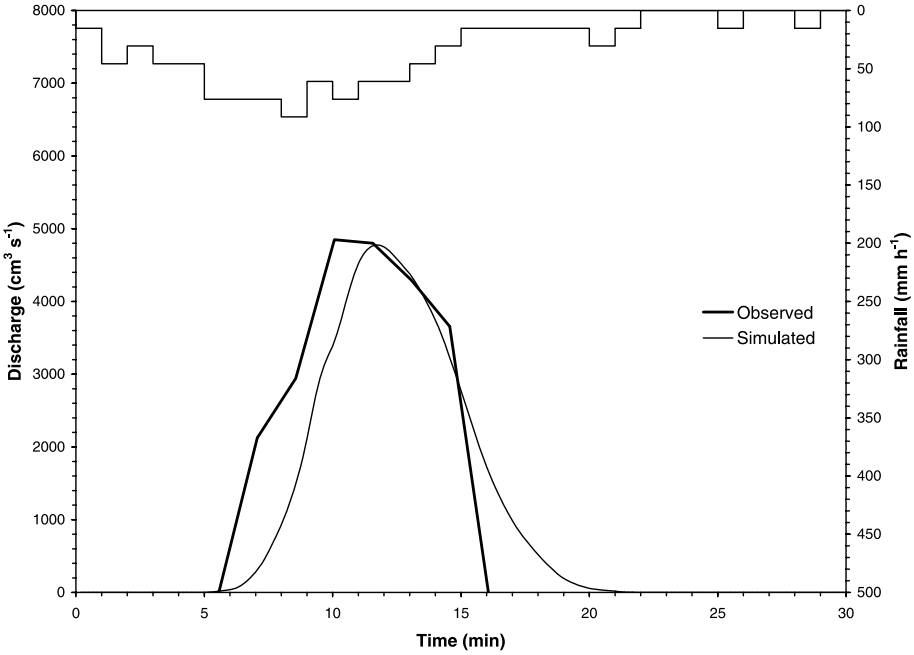

Fig. 9. North watershed observed and simulated hydrographs for the August 12, 1998 storm.

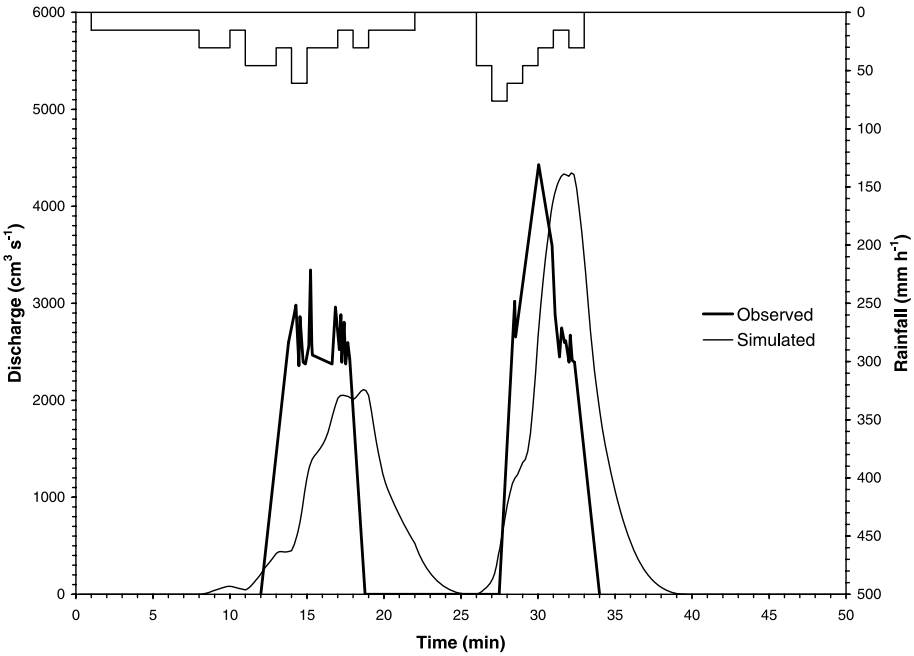

Fig. 10. South watershed observed and simulated hydrographs for the August 14, 1997 storm.

7. Runon infiltration under shrubs

7.1. Introduction

One of the approaches employed in the Jornada LTER project to study the transition from grassland to shrubland involved computer modeling based on a hierarchy of ecosystem functional types (EFTs) (Reynolds et al., 1997). In this approach, a landscape is represented by square cells known as patch EFTs, or simply patches. All patches in a landscape representation are equal in size, but the patch area may range from 1 to 10 m^2. Aggregations of patches, from 1 ha to 1 km^2, were referred to as patch mosaic EFTs. For modeling the process of desertification in the Jornada Basin, Reynolds et al. (1997) classified patches as either grass, shrub, or bare soil (Fig. 11); and grass, mixed, and shrub mosaics were defined to correspond to the stages observed in the transition from grassland to shrubland.

The growth of vegetation within patches has been modeled by the Patch AridLands Simulator (PALS) (Reynolds et al., 1992), but the lateral movements of water and nutrients within and between patches have not been taken into account. This is because runoff models that can simulate overland flow in semiarid environments are unable to operate at the scale of an individual patch. Although field studies have indicated that lateral movements of water and nutrients are important in ecosystem function (e.g., Schlesinger and Jones, 1984; Noy-Meir, 1985), no quantitative investigation of their importance has hitherto been undertaken. Against this background, a 2D model has been developed in this study that is capable of simulating lateral movements of water and nutrients at the scale of an individual patch.

Water that infiltrates into the soil at the base of a shrub may be either rain infiltration or runon infiltration. Rain infiltration refers to the infiltration of water that arrives at the base of a shrub from above in the form of either stemflow, leaf drip, or throughfall (i.e., rainfall passing directly through the canopy onto the surface of the soil) (Martinez-Meza and Whitford, 1996; Whitford et al., 1997). In contrast, runon infiltration refers to the infiltration of water that arrives at the base of a shrub as overland flow from the adjacent intershrub area. Little is known about the relative importance of these two types of infiltration, mainly because they are extremely difficult to distinguish in the field.

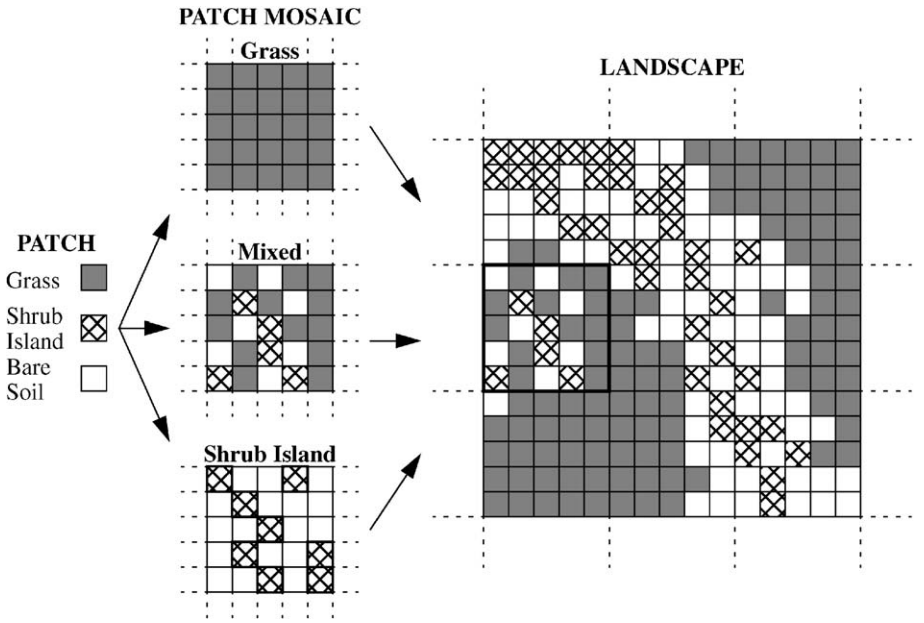

Fig. 11. Patch, patch mosaic, and landscape ecosystem function types (EFTs) (Reynolds et al., 1997).

Table 6
Model parameter values used in runon simulation runs

Watershed	Surface type	$E(K_s)$ (cm h^{-1})	CV (K_s)	B (cm)	F_i (cm)	ff
North	Intershrub	2.10[a]	0.19	1.22	1.68[a]	0.73
	Shrub-bare	6.58	0.17	0.55	1.68	0.73
	Shrub-grass	8.82	0.20	0.10	1.68	1.00
	Shrub-litter	8.04	0.43	0.13	1.68	1.37
South	Intershrub	1.35[a]	0.74	1.77	1.51[a]	0.58
	Shrub	6.49	0.38	0.63	1.51	0.38

[a] Values of K_s and F_i for the intershrub surface are the mean values for the storms with initially wet soil (i.e., three out of the four storms at the north watershed—the July 22, 1998, storm is excluded—and both of the storms at the south watershed).

However, the problem can be addressed using computer modeling.

The relative importance of runon infiltration in supplying water to shrubs can be quantified by expressing the depth of runon infiltration as a percentage of the total depth of infiltration in a cell. In the following section, simulations are performed to investigate how the mean percentage of runon infiltration for all shrub cells in a watershed varies with rainfall and antecedent soil moisture conditions.

7.2. Model simulations

Model simulations were performed for the north and south watersheds using the set of parameter values given in Table 6. The values of $E(K_s)$, CV(K_s) and F_i listed in the table are discussed below. The values of B and ff are the same as those used in the calibration runs described in Section 6.6.

7.2.1. Rainfall

The effect of the rate and variability of rainfall on the relative importance of runon infiltration was examined by simulating a series of 30-min storms using seven mean rainfall rates $\bar{r}$. As shown in Table 7, 30-min storms with this range of intensities correspond to recurrence intervals ranging from 2 to over 100 years. For each $\bar{r}$, two temporal rainfall patterns were simulated: (i) constant rainfall at $\bar{r}$ for 30 min and (ii) a simple pattern in which the rainfall rate r varies about as follows:

$0 - 6$ min $\quad \bar{r} - 1$ cm h^{-1}

$6.01 - 12$ min $\quad \bar{r}$

$12.01 - 18$ min $\quad \bar{r} + 2$ cm h^{-1}

$18.01 - 24$ min $\quad \bar{r}$

$24.01 - 30$ min $\quad \bar{r} - 1$ cm h^{-1}

7.2.2. Antecedent soil moisture

Typical wet antecedent soil moisture conditions were represented in each watershed by setting F_i equal to its mean value from the calibration runs for the watershed (Table 6). For the north watershed, F_i was based on values for only three out of the four storms, the July 22, 1998 storm being excluded because the soil was dry prior to the storm. In order to investigate the effect of wet antecedent soil conditions on the relative importance of runon infiltration, each simulation run was repeated with F_i set equal to 0.01 cm to represent dry soil.

7.2.3. Saturated hydraulic conductivity

For the calibration runs, the value of K_s was constant for all cells of a given surface type; but because runon infiltration occurs as a consequence of spatial variability in K_s, it was necessary in this part of the study to incorporate a degree of spatial variability into the values of K_s assigned to model cells. In accordance with other modeling studies (e.g., Smith and Hebbert, 1979; Woolhiser et al., 1996; Corradini et al., 1998), values of K_s were assigned to model cells at random from a lognormal distribution with mean

Table 7
Rainfall and antecedent soil moisture conditions

Mean rainfall rate r (cm h^{-1})	Recurrence interval for 30-min event[a] (year)	Temporal variability of rainfall	Antecedent soil moisture conditions
4.0	2	Constant	Dry ($F_i = 0.01$ cm)
			Wet[b]
		Variable	Dry ($F_i = 0.01$ cm)
			Wet[b]
4.5		repeat as above	repeat as above
5.0	10		
5.5			
6.0	25–50		
6.5			
7.0	100		

[a] Data from Miller et al. (1973) and Abrahams et al. (in press).
[b] The values of F_i used to represent wet antecedent soil moisture conditions in each watershed are listed in Table 6.

$E(K_s)$ and coefficient of variation CV(K_s) (Nielsen et al., 1973; Baker and Bouma, 1976). A different distribution was used for each surface type using the $E(K_s)$ and CV(K_s) listed in Table 6. The values of $E(K_s)$ are the mean values of K_s for the calibration runs, and the values of CV(K_s) are based on the K_s values obtained for each surface type from the runoff plot experiments.

The inclusion of a stochastic element in the modeling may appear to be inconsistent with the objective of this study, which is to develop a deterministic runoff model. The reason for not incorporating spatial variability into K_s in the model calibration runs is that the aim of these runs was to achieve as close a match as possible between observed and simulated hydrographs. Because the runoff hydrograph is particularly sensitive to variation in CV(K_s), it would have been necessary to specify values of CV(K_s) with a level of certainty that could not be achieved on the basis of the number of runoff plot experiments performed for each watershed. In this part of the study, the aim was to perform model simulations using a more general set of soil conditions. Therefore, while it is necessary to ensure that these conditions are realistic, precise specification of CV(K_s) is not as essential as it is for the calibration runs.

7.3. Simulation results

The simulation results are presented as graphs of the mean percentage of runon infiltration in shrub cells against $\bar{r}$ (Figs. 12–16). Each graph consists of four curves corresponding to the four simulated cases: constant r and initially dry soil; constant r and initially wet soil; variable r and initially dry soil; and variable r and initially wet soil.

Although the curves for the north watershed (Fig. 12) are similar to those for the south watershed (Fig. 13), the mean runon percentages are slightly higher for the north watershed, which implies that runon infiltration is more important in this watershed. For both watersheds, the lowest mean runon percentages are associated with an initially dry soil and are relatively insensitive to $\bar{r}$. In contrast, the mean runon percentages for an initially wet soil are inversely proportional to $\bar{r}$, with the largest values being associated with a variable rainfall pattern. Although the mean runon percentages shown in the curves are

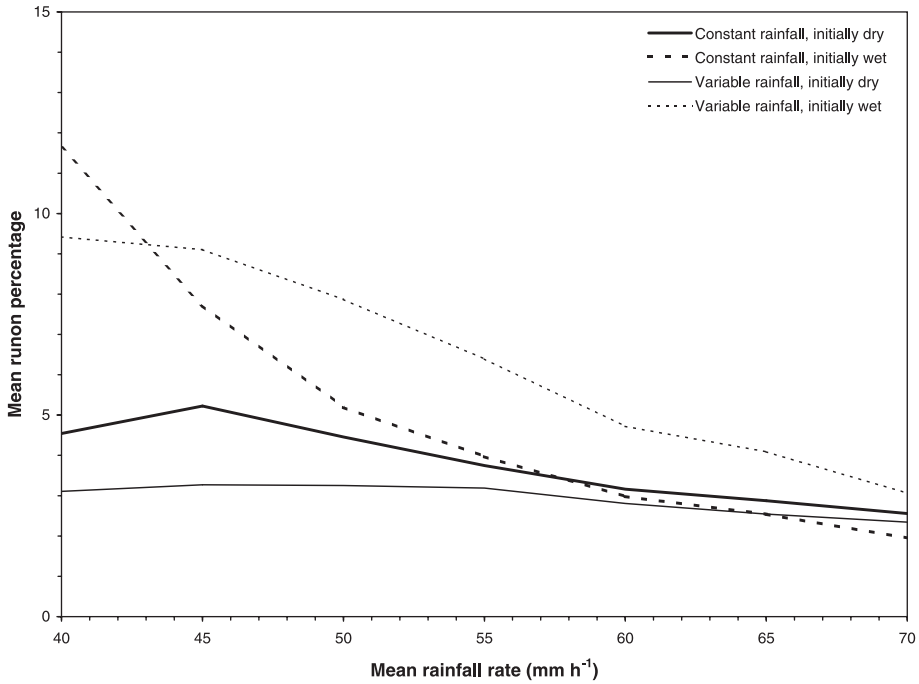

Fig 12. Graph of mean runon percentage against mean rainfall rate for north watershed shrub cells (N = 147).

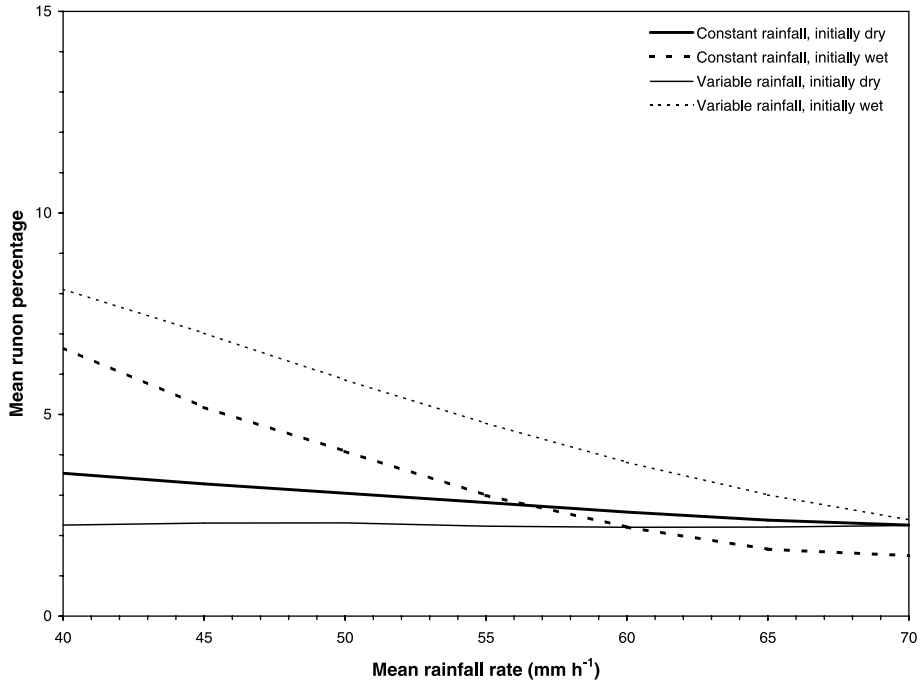

Fig. 13. Graph of mean runon percentage against mean rainfall rate for south watershed shrub cells ($N=286$).

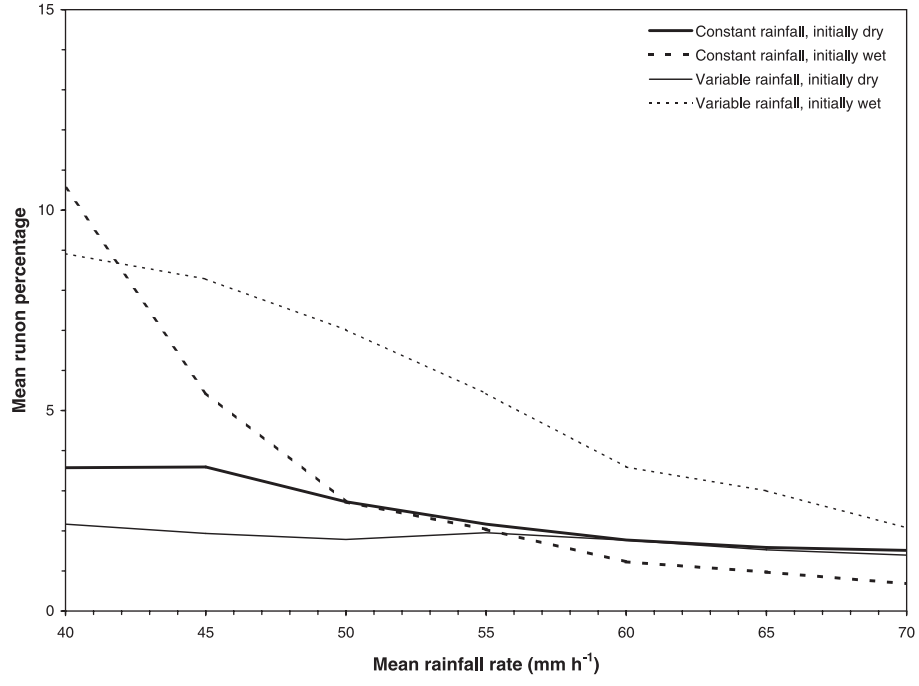

Fig. 14. Graph of mean runon percentage against mean rainfall rate for north watershed shrub-bare cells ($N=86$).

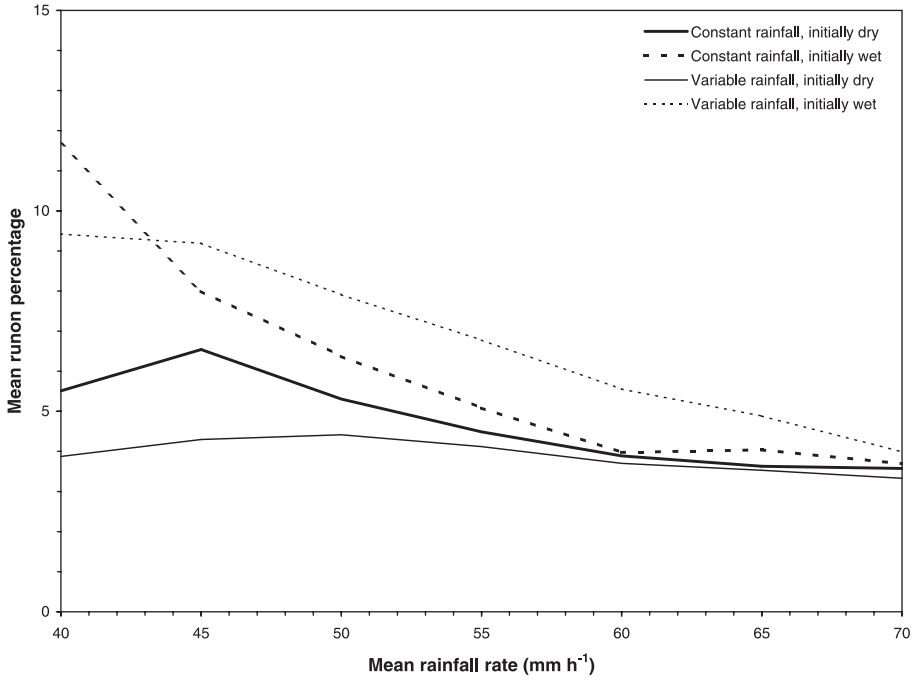

Fig. 15. Graph of mean runon percentage against mean rainfall rate for north watershed shrub-litter cells ($N=44$).

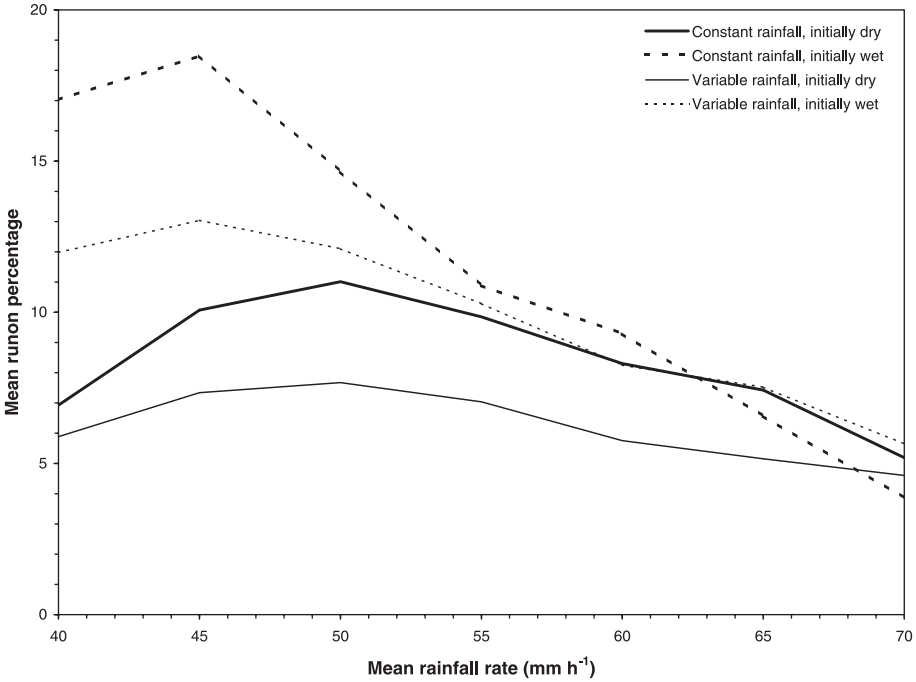

Fig. 16. Graph of mean runon percentage against mean rainfall rate for north watershed shrub-grass cells ($N=17$).

relatively low (3–12% of total infiltration in the north watershed and 2–8% of total infiltration in the south watershed), their range is high. For each watershed, the maximum runon percentages are associated with constant rainfall and an initially wet soil and vary between about 50% at low r to about 30% for high r in each watershed.

The trends described above can be partially explained as follows. When $\bar{r}$ is low, cells do not reach saturation quickly, and they frequently have excess infiltration capacity that may be satisfied wholly or partly by runon infiltration. The potential for runon infiltration is greatest when the soil is initially wet because ponding and, hence, runoff occurs earlier in all cells (shrub and intershrub) than it would if the soil were initially dry. In contrast, when $\bar{r}$ is high, the soil quickly becomes saturated, regardless of whether the soil is initially wet or dry. As a consequence, little runon infiltration occurs.

The higher mean runon percentages for the north watershed are due in part to the higher $E(K_s)$ for the shrub cells in this watershed. The relation between $E(K_s)$ and the nature of the curves can be illustrated by considering each surface type separately in order of increasing $E(K_s)$. Figs. 14–16 show the curves for shrub-bare cells ($E(K_s) = 6.58$ cm h^{-1}), shrub-litter cells ($E(K_s) = 8.04$ cm h^{-1}), and shrub-grass cells ($E(K_s) = 8.82$ cm h^{-1}), respectively. As these diagrams show, the mean runon percentages increase with $E(K_s)$, with the effect being greatest at low $\bar{r}$ and weakening with $\bar{r}$. The reason for the reversal in the relative positions of the two curves corresponding to wet initial conditions in Fig. 16 is not clear.

Many factors determine the relative importance of runon infiltration. In particular, the degree of spatial variability in K_s and the spatial pattern of K_s affect the relative importance of runon infiltration through their control over the generation of both runoff and infiltration. For example, if K_s decreases along a flow path leading to a shrub, the amount of runon that may arrive at the shrub and be available to infiltrate will be less than if K_s increases along the flow path (e.g., Woolhiser et al., 1996).

The relative importance of runon infiltration in shrub cells also depends on the topography and the position of the shrubs with respect to flow paths within the watershed. Shrubs often reside on microtopographic mounds a few centimeters high, which means that runon infiltration will not occur unless the flow has sufficient depth. Because the difference in elevation between the shrub mounds and the surrounding intershrub area is greater in the south watershed (Fig. 3) than in the north watershed (Fig. 2), it may be inferred that shrubs in the south watershed will receive less runon infiltration than those in the north watershed. The simulation results support this inference.

7.4. Discussion

Although the investigation of runon infiltration described above is based on a limited number of simulation runs, the results are consistent with the findings of ecologists with respect to the relation between plant function and rainfall conditions. Creosotebushes exhibit maximal rates of shoot and root growth in late spring (Reynolds et al., 1999) at the end of the winter/spring rainfall season (October 1 to May 31). As Figs. 12–16 show, the role of runon infiltration in supplying water to shrubs is greatest for low-intensity rainfall events that are typical of this season. In contrast, runon infiltration is relatively ineffective during the summer, when high-intensity storms saturate the surface layer of the soil.

With respect to different surface types, the results show that runon infiltration is more important for shrubs that have grass at their base than it is for shrubs that have bare soil or litter at their base. This finding is attributed to the dense matrix of roots under the grass that create macropores that promote infiltration.

The extent to which the water supplied to a shrub is due to runon depends on many interrelated factors. In this study, it has only been possible to explore some of these factors. However, the results suggest that a much broader study of the role of runon infiltration in supplying water and nutrients to shrubs would be worthwhile. Although the mean percentages of runon infiltration are quite low for the conditions simulated in this investigation, they are sufficiently large to suggest that lateral flows must be taken into account in studies of shrubland ecosystems.

8. Conclusion

A new 2D distributed parameter model was developed to simulate overland flow during individual

rainfall events in two semiarid shrubland watersheds in the Jornada Basin, New Mexico. The model is based on the kinematic approximation to the dynamic Saint Venant equations and operates at the scale of the individual shrub. Each watershed is therefore represented as a matrix of 1-m^2 cells. These cells are classified as either shrub or intershrub to reflect the different hydrologic properties of these surfaces. In the model, flow velocity is computed using the Darcy–Weisbach flow equation, and infiltration capacity is computed using the Smith–Parlange infiltration equation. The model has only six parameters: slope s, rainfall rate r, saturated hydraulic conductivity K_s, a soil storage parameter B, *friction factor ff*, and initial infiltrated depth F_i. The values of s were determined from DEMs based on detailed watershed surveys. Data on r were obtained from tipping bucket rain gauges, while values of K_s and B for shrub and intershrub surfaces in each watershed were computed from rainfall simulation experiments on runoff plots of the same size as the model cells (i.e., 1 m^2). Values of *ff* for the intershrub surfaces were calculated from a separate set of rainfall simulation experiments, which also included trickle flow to simulate runon from upslope areas. Since data on antecedent soil moisture were unavailable, the initial value of infiltrated depth F_i in all cells was set equal to the depth of rainfall during the 24 h prior to the storm.

The model was initially applied to each watershed to simulate runoff caused by a storm that occurred on July 30, 1997. The model underpredicted runoff from the two watersheds because the measured values of K_s were too high compared to actual values for the storm. The discrepancies between the measured and actual K_s values are attributed to surface sealing, which reduces K_s. The rainfall simulation experiments were conducted at the beginning of summer after several months without rain. At that time, the surface seals were badly degraded by drying, cracking, and animal digging. In contrast, rainfall immediately prior to the July 30 storm had enhanced seal development and so the K_s values were lower for the storm than for the simulated rainstorms. Close matches between the observed and simulated hydrographs could be obtained by reducing K_s for the intershrub areas to account for such sealing.

Although the model could not be validated, it can be used to improve understanding of the hydrologic processes that operate in semiarid shrubland environments, such as the role of runon infiltration in supplying water to shrubs. The relative importance of runon infiltration in supplying water to shrubs was examined by performing a series of model simulations. Wet and dry antecedent soil moisture conditions in each watershed were simulated for a range of rainfall conditions typical of the Jornada Basin, and each cell was assigned a value of K_s at random from a lognormal distribution.

The simulations revealed that the mean runon percentage (i.e., the depth of runon infiltration expressed as a percentage of the total depth of infiltration in a cell) for all shrub cells varied with mean rainfall rate $\bar{r}$ in a similar manner in both watersheds. The highest mean runon percentages were associated with an initially wet soil, a variable rainfall pattern, and low $\bar{r}$. Runon infiltration was found to be more important in the north watershed than in the south watershed due (i) to the higher values of K_s in the north watershed and (ii) to the greater difference in elevation between shrub mounds and intershrub areas in the south watershed. The mean runon percentages were found to be sufficiently large to suggest (i) that lateral flows must be taken into account in studies of shrubland ecosystems and (ii) that a much broader study of the role of runon infiltration in supplying water to shrubs is warranted.

Acknowledgements

This research was supported by the National Science Foundation Jornada Basin Long-Term Ecological Research (LTER) project (DEB 94-11971) and the National Center for Geographic Information and Analysis (SBR 88-10917), University at Buffalo, The State University of New York. We are grateful to Bruce Pitman, Department of Mathematics, University at Buffalo, for his invaluable assistance in the development of the model; to John Anderson and the LTER technicians at New Mexico State University, Las Cruces, for operating and maintaining the hydrometeorological instruments in the two watersheds; to Kris Havstad and staff at the USDA-ARS Jornada Experimental Range for building the supercritical flumes and providing the tanker truck; and to Melissa Neave, Scott Rayburg, and Scott McCabe,

University at Buffalo, for their assistance with the field work.

References

Abrahams, A.D., Parsons, A.J., 1990. Determining the mean flow depth of overland flow in field studies of flow hydraulics. Water Resources Research 26, 501–503.

Abrahams, A.D., Parsons, A.J., 1994. Hydraulics of interrill overland flow on stone-covered desert surfaces. Catena 23, 111–140.

Abrahams, A.D., Parsons, A.J., Luk, S.-H., 1986. Resistance to overland flow on desert hillslopes. Journal of Hydrology 88, 343–363.

Abrahams, A.D., Parsons, A.J., Luk, S.-H., 1990. Field experiments on the resistance to overland flow on desert hillslopes. In: Walling, D.E., Yair, A., Berkowicz, S. (Eds.), Erosion, Transport and Deposition Processes. IAHS Publication, vol. 189. IAHS Press, Wallingford, UK, pp. 1–18.

Abrahams, A.D., Parsons, A.J., Wainwright, J., 1994. Resistance to overland flow on semiarid grassland and shrubland hillslopes, Walnut Gulch, southern Arizona. Journal of Hydrology 156, 431–446.

Abrahams, A.D., Parsons, A.J., Wainwright, J., 1995. Effects of vegetation change on interrill runoff and erosion, Walnut Gulch, southern Arizona. Geomorphology 13, 37–48.

Abrahams, A.D., Neave, M., Schlesinger, W.H., Wainwright, J., Howes, D.A., Parsons, A.J., in press. In: Schlesinger, W.H., Huenneke, L., Havstad, K. (Eds.), Fluxes of Water and Materials: Processes and Controls. Jornada. Oxford Univ. Press, Oxford, UK.

Abrahams, A.D., Parsons, A.J., Wainwright, J., manuscript in preparation. Disposition of stemflow under creosotebush.

Archer, S., Scifres, C., Bassham, C.R., Maggio, R., 1988. Autogenic succession in a subtropical savanna: conversion of grassland to thorn woodland. Ecological Monographs 58, 111–127.

Baird, A.J., 1997. Overland flow generation and sediment mobilisation by water. In: Thomas, D.S.G. (Ed.), Arid Zone Geomorphology: Process, Form and Change in Drylands, 2nd ed. Wiley, NY, pp. 153–215.

Baker, F.G., Bouma, J., 1976. Variability of hydraulic conductivity in two subsurface horizons of two silt loam soils. Soil Science Society of America Journal 40, 219–222.

Bathurst, J.T., 1986. Physically-based distributed modelling of an upland catchment using the Système Hydrologique Européen. Journal of Hydrology 87, 79–102.

Beven, K., 1989. Changing ideas in hydrology—the case of physically-based models. Journal of Hydrology 105, 157–172.

Buffington, L.C., Herbel, C.H., 1965. Vegetation changes on a semidesert grassland range from 1858 to 1963. Ecological Monographs 35, 139–164.

Carson, M.A., Kirkby, M.J., 1972. Hillslope Form and Process Cambridge Univ. Press, Cambridge, UK, 475 pp.

Chow, V.T., 1959. Open Channel Hydraulics McGraw-Hill, London. 680 pp.

Corradini, C., Morbidelli, R., Melone, F., 1998. On the interaction between infiltration and Hortonian runoff. Journal of Hydrology 204, 52–67.

Cundy, T.W., Tento, S.W., 1985. Solution to the kinematic wave approach to overland flow routing with rainfall excess given by Philip's equation. Water Resources Research 21, 1132–1140.

Davis, S.F., 1988. Simplified second-order Godunov-type methods. SIAM Journal of Scientific and Statistical Computing 9, 445–473.

de Saint Venant, B., 1871. Theory of unsteady water flow, with application to river floods and to propagation of tides in river channels. French Academy of Science 73.

Dunne, T., Zhang, W., Aubry, B.F., 1991. Effects of rainfall, vegetation, and microtopography on infiltration and runoff. Water Resources Research 27, 2271–2285.

Emmett, W.W., 1970. The hydraulics of overland flow on hillslopes. United States Geological Survey Professional Paper 662-A.

Emmett, W.W., 1978. Overland flow. In: Kirkby, M.J. (Ed.), Hillslope Hydrology. Wiley, Chichester, UK, pp. 145–176.

Environmental Systems Research Institute, 1998. ArcInfo User Manual. Redlands, CA.

Flanagan, D.C., Nearing, M.A. (Eds.), 1995. USDA—Water Erosion Prediction Project Hillslope Profile and Watershed Model Documentation, NSERL Report 10. National Soil Erosion Laboratory, West Lafayette, IN.

Freeze, R.A., 1980. A stochastic–conceptual analysis of rainfall–runoff processes on a hillslope. Water Resources Research 16, 391–408.

Freund, R.J.J., Littell, R.C., 1991. SAS System for Regression, 2nd ed. SAS Publ., Cary, NC. 232 pp.

Gibbens, R.P., Beck, R.F., 1988. Changes in grass basal area and forb densities over a 64-year period on grassland types of the Jornada Experimental Range. Journal of Range Management 41, 186–192.

Gilley, J.E., Weltz, M.A., 1995. Hydraulics of overland flow. In: Flanagan, D.C., Nearing, M.A. (Eds.), USDA-Water Erosion Prediction Project Hillslope Profile and Watershed Model Documentation. NSERL Report 10. National Soil Erosion Research Laboratory, West Lafayette, IN, pp. 10.1–10.7.

Goodrich, D.C., 1990. Geometric simplification of a distributed rainfall–runoff model over a large range of basin scales. PhD dissertation, University of Arizona, Tucson. 361 pp.

Goodrich, D.C., 1991. Basin scale and runoff model complexity. Department of Hydrology and Water Resources Technical Report HWR 91-010, University of Arizona, Tucson. 361 pp.

Grayson, R.B., Moore, I.D., McMahon, T.A., 1992a. Physically based hydrologic modeling: 1. A terrain-based model for investigative purposes. Water Resources Research 28, 2639–2658.

Grayson, R.B., Moore, I.D., McMahon, T.A., 1992b. Physically based hydrologic modeling: 2. Is the concept realistic? Water Resources Research 28, 2659–2666.

Green, W.H., Ampt, G.A., 1911. Studies on soil physics: 1. The flow of air and water through soils. Journal of Agricultural Science 4, 1–24.

Hawkins, R.H., Cundy, T.W., 1987. Steady-state analysis of infiltration and overland flow for spatially-varied hillslopes. Water Resources Bulletin 23, 251–256.

Henderson, F.M., Wooding, R.A., 1964. Overland flow and groundwater flow from a steady rainfall of finite duration. Journal of Geophysical Research 69, 1531–1540.

Horton, R.E., 1933. The role of infiltration in the hydrologic cycle. Transactions of the American Geophysical Union 14, 446–460.

Li, G., Abrahams, A.D., 1999. Controls of sediment transport capacity in laminar interrill flow on stone-covered surfaces. Water Resources Research 35, 305–310.

Lighthill, M.J., Witham, G.B., 1955. On kinematic waves: 1. Flood movement in long rivers. Proceedings of the Royal Society A229, 281–316.

Luk, S.H., Abrahams, A.D., Parsons, A.J., 1986. A simple rainfall simulator and trickle system for hydro-geomorphological experiments. Physical Geography 7, 344–356.

Martinez-Meza, E., Whitford, W.G., 1996. Stemflow, throughfall and channelization of stemflow by roots in three Chihuahuan desert shrubs. Journal of Arid Environments 32, 271–287.

McIntyre, D.S., 1958. Permeability measurements of soil crusts formed by raindrop impact. Soil Science 85, 185–189.

Miller, J.F., Frederick, R.H., Tracey, R.J., 1973. Precipitation-Frequency Atlas of the Western United States, Volume IV—New Mexico, NOAA Atlas 2. U.S. Department of Commerce Publication, Silver Spring, MD.

Mohammed, D., Kohl, R.A., 1987. Infiltration response to kinetic energy. Transactions of the American Society of Agricultural Engineers 30, 108–109.

Moore, I.D., 1981. Effect of surface sealing on infiltration. Transactions of the American Society of Agricultural Engineers 24, 1546–1552.

Moore, I.D., Grayson, R.B., 1991. Terrain-based catchment partitioning and runoff prediction using vector elevation data. Water Resources Research 27, 1177–1191.

Navar, J., Bryan, R., 1990. Interception loss and rainfall redistribution by three semi-arid growing shrubs in northeastern Mexico. Journal of Hydrology 115, 51–63.

Neave, M., in press. Impact of small mammal disturbances on runoff and sediment yield from grassland and shrubland ecosystems in the Chihuahuan Desert. Catena.

Nielsen, D.R., Biggar, J.W., Erh, K.T., 1973. Spatial variability of field measured soil–water properties. Hilgardia 42, 215–260.

Noy-Meir, I., 1985. Desert ecosystem structure and function. In: Evanari, M., Noy-Meir, I., Goodall, D.W. (Eds.), Hot Deserts and Arid Shrublands. Elsevier, Amsterdam, pp. 93–103.

Parsons, A.J., Abrahams, A.D., Simanton, J.R., 1992. Microtopography and soil-surface materials on semi-arid hillslopes, southern Arizona. Journal of Arid Environments 22, 107–115.

Parsons, A.J., Wainwright, J., Abrahams, A.D., Simanton, J.R., 1997. Distributed dynamic modelling of interrill overland flow. Hydrological Processes 11, 1838–1859.

Pickup, G., 1988. Hydrology and sediment models. In: Anderson, M.G. (Ed.), Modelling Geomorphological Systems. Wiley, NY, pp. 153–215.

Poesen, J.W.A., 1987. The role of slope angle in surface seal formation. In: Gardiner, V. (Ed.), International Geomorphology 1986. Part II. Wiley, Chichester, UK, pp. 437–448.

Poesen, J.W.A., 1992. Mechanisms of overland-flow generation and sediment production on loamy sand soils and sandy soils with and without rock fragments. In: Parsons, A.J., Abrahams, A.D. (Eds.), Overland Flow: Hydraulics and Erosion Mechanics. UCL Press, London, UK, pp. 275–305.

Ponce, V.M., 1991. The kinematic wave controversy. Journal of Hydraulic Engineering 117, 511–525.

Refsgaard, J.C., 1997. Parameterisation, calibration and validation of distributed hydrological models. Journal of Hydrology 198, 69–97.

Refsgaard, J.C., Storm, B., 1996. Construction, calibration and validation of hydrological models. In: Abbott, M.B., Refsgaard, J.C. (Eds.), Distributed Hydrological Modelling. Kluwer Academic Publishing, Dordrecht, The Netherlands, pp. 41–54.

Reynolds, J.F., Hilbert, D.W., Chen, J.-L., Harley, P.C., Kemp, P.R., Leadley, P.W., 1992. Modeling the Response of Plants and Ecosystems to Elevated CO_2 and Climatic Change, DOE/ER-60490T-HI. National Technical Information Service, U.S. Department of Commerce, Springfield, VA.

Reynolds, J.F., Virginia, R.A., Schlesinger, W.H., 1997. Defining functional types for models of desertification. In: Smith, T.M., Shugart, H.H., Woodward, F.I. (Eds.), Plant Functional Types: Their Relevance to Ecosystem Properties and Global Change. Cambridge Univ. Press, Cambridge, UK, pp. 194–214.

Reynolds, J.F., Virginia, R.A., Kemp, P.A., de Soyza, A.G., Tremmel, D.C., 1999. Impact of drought on desert shrubs: effects of seasonality and degree of resource island development. Ecological Monographs 69, 69–106.

Römkens, M.J.M., Prasad, S.N., Whisler, F.D., 1990. Surface sealing and infiltration. In: Anderson, M.G., Burt, T.P. (Eds.), Process Studies in Hillslope Hydrology. Wiley, NY, pp. 127–172.

Schlesinger, W.H., Jones, C.S., 1984. The comparative importance of overland runoff and mean annual rainfall to shrub communities of the Mojave Desert. Botanical Gazette 145, 116–124.

Schlesinger, W.H., Pilmanis, A.M., 1998. Plant–soil interactions in deserts. Biogeochemistry 42, 169–187.

Schlesinger, W.H., Reynolds, J.F., Cunningham, G.L., Huenneke, L.F., Jarrell, W.M., Virginia, R.A., Whitford, W.G., 1990. Biological feedbacks in global desertification. Science 247, 1043–1048.

Schlesinger, W.H., Abrahams, A.D., Parsons, A.J., Wainwright, J., 1999. Nutrient losses in runoff from grassland and shrubland habitats in southern New Mexico: 1. Rainfall simulation experiments. Biogeochemistry 45, 21–34.

Schmid, B.H., 1989. On overland flow modelling: can rainfall excess be treated as independent of flow depth? Journal of Hydrology 107, 1–8.

Scoging, H.M., Thornes, J.B., 1979. Infiltration characteristics in a semiarid environment. In: Hydrology of Areas of Low Precipitation. Intern. Assoc. Hydrol. Sci. Publ. 128. IAHS Press, Wallingford, UK, pp. 159–168.

Scoging, H.M., Parsons, A.J., Abrahams, A.D., 1992. Application of a dynamic overland-flow hydraulic model to a semi-arid hillslope, Walnut Gulch, Arizona. In: Parsons, A.J., Abrahams, A.D. (Eds.), Overland Flow Hydraulics and Erosion Mechanics. UCL Press, London, UK, pp. 105–145.

Sherman, B., Singh, V.P., 1976. A distributed converging overland flow model: 1. Mathematical solutions. Water Resources Research 12, 889–896.

Smith, R.E., Hebbert, R.H.B., 1979. A Monte Carlo analysis of the hydrologic effects of spatial variability of infiltration. Water Resources Research 15, 419–429.

Smith, R.E., Parlange, J.-Y., 1978. A parameter-efficient hydrologic infiltration model. Water Resources Research 14, 533–538.

Smith, R.E., Goodrich, D.G., Woolhiser, D.A., Unkrich, C.L., 1995. KINEROS—a KINematic runoff and EROSion model. In: Singh, V.P. (Ed.), Computer Models of Watershed Hydrology. Water Resources Publications, Fort Collins, CO, pp. 697–732.

Springer, E.P., Cundy, T.W., 1987. Field scale evaluation of infiltration parameters from soil texture for hydrologic analysis. Water Resources Research 23, 325–341.

Tarboton, D.G., 1997. A new method for the determination of flow directions and upslope areas in grid digital elevation models. Water Resources Research 33, 309–319.

Thompson, A.L., James, L.G., 1985. Water droplet impact and its effect on infiltration. Transactions of the American Society of Agricultural Engineers 28, 1506–1510.

Vertessy, R.A., Hatton, T.J., O'Shaughnessy, P.J., Jayasuriya, M.D.A., 1993. Predicting water yield from a mountain ash forest catchment using a terrain analysis based catchment model. Journal of Hydrology 150, 665–700.

Wainwright, J., in press. Climate and climatic variability at Jornada. In: Schlesinger, W.H., Huenneke, L., Havstad, K. (Eds.), Jornada. Oxford Univ. Press, Oxford, UK.

Wainwright, J., Parsons, A.J., Abrahams, A.D., 1999. Rainfall energy under creosotebush. Journal of Arid Environments 43, 111–120.

Whitford, W.G., Anderson, J., Rice, P.M., 1997. Stemflow contribution to the 'fertile island' effect in creosotebush. Journal of Arid Environments 35, 451–457.

Woolhiser, D.A., Liggett, J.A., 1967. Unsteady one-dimensional flow over a plane: the rising hydrograph. Water Resources Research 3, 753–771.

Woolhiser, D.A., Smith, R.E., Goodrich, D.C., 1990. KINEROS: A Kinematic Runoff and Erosion Model: Documentation and User Manual, U.S. Department of Agriculture, Agricultural Research Service Report No. 77. Fort Collins, CO.

Woolhiser, D.A., Smith, R.E., Giraldez, J.-V., 1996. Effects of spatial variability of saturated hydraulic conductivity on Hortonian overland flow. Water Resources Research 32, 671–678.

Wu, Y.-H., Yevjevich, V., Woolhiser, D.A., 1978. Effects of Surface Roughness and its Spatial Distribution on Runoff Hydrographs. Hydrological Papers, vol. 96. Colorado State University, Fort Collins, CO. 47 pp.

Zhang, W., Cundy, T.W., 1989. Modeling of two-dimensional overland flow. Water Resources Research 25, 2019–2035.